Coastal and regional marine heatwaves and cold-spells in the Northeast Atlantic

Amélie Simon[1*], Coline Poppeschi[2], Sandra Plecha[1], Guillaume Charria[2], Ana Russo[1]

[1] Universidade de Lisboa, Faculdade de Ciências, Instituto Dom Luiz (IDL), 1749-016, Lisboa, Portugal
[2] Ifremer, Univ. Brest, CNRS, IRD, Laboratory for Ocean Physics and Satellite remote sensing (LOPS), IUEM, 29280 Brest, France

*corresponding author: Dr. Amélie Simon; ajsimon@fc.ul.pt

Abstract

The latest IPCC report describes an increase in the number and intensity of marine heatwaves (MHWs) and a decrease in marine cold-spells (MCSs) in the global ocean. However, these reported changes are not uniform on a regional to local basis and it remains unknown if coastal areas follow the open ocean trends. Ocean temperature measurements collected by satellites (from 1982-2022) and 13 coastal buoys (from 1990-2022) are analyzed in the Northeast Atlantic and three subregions: English Channel, Bay of Brest and Bay of Biscay. The activity metric, combining the number of events, intensity, duration and spatial extent, is used to evaluate the magnitude of these extreme events. The results from *in situ* and satellite datasets for each of the studied regions are quite in agreement, although the satellite dataset underestimates the amplitude of activity for both MHWs and MCS. This supports the applicability of the method to both *in situ* and satellite data, albeit with caution on the amplitude of these events. Also, this localized study in European coastal Northeast Atlantic water highlights that similar changes are being seen in coastal and open oceans regarding extreme events of temperature, with MHWs being more frequent, longer, and extending over larger areas, while the opposite is seen for MCSs. These trends can be explained by changes in both the mean and variance of sea-surface temperature. Besides, the pace of evolution and dynamics of marine extreme events differs among the subregions. Among the three studied subregions, the English Channel is the region experiencing the strongest increase in summer MHWs activity over the last four decades. Summer MHWs were very active in the English Channel in 2022 due to long events, in the Bay of Biscay in 2018 due to intense events and in the Bay of Brest in 2017 due to a high occurrence of events. Winter MCSs were the largest in 1987 and 1986 due to long and intense events in the English Channel. Finally, our findings suggest that at an interannual time scale, the positive North Atlantic Oscillation favors the generation of strong summer MHWs in the Northeast Atlantic, while dominant low-pressure conditions over Northern Europe and a high off the Iberian Peninsula in winter dominates for MCSs. A preliminary analysis of air-sea heat flux suggests that, in this region, low cloud coverage is a key parameter for the generation of summer MHWs while strong winds and high cloud coverage is important for the apparition of winter MCSs.

Keywords

Extreme events, Sea Surface Temperature, Long-term *in situ* observations, Satellite data, Marine heatwaves, Marine cold-spells, Bay of Biscay, English Channel, North Atlantic Oscillation

1. Introduction

Heatwaves and cold-spells are extreme events in which there is a strong anomaly in temperature for a certain period which can occur at a regional spatial scale. This type of phenomenon can occur both in the atmosphere and in the ocean, with remarkable consequences both for terrestrial and marine ecosystems (Ruthrof et al., 2018). In the case of marine events (hereafter referred to as marine heatwaves (MHWs) or marine cold-spells (MCSs)), severe large-scale biodiversity losses may occur such as species extinction, habitat destruction and abrupt changes in the geographical distribution and structure of communities, as well as the nutrient cycle (Frölicher and Laufkötter, 2018; Ruthrof et al., 2018; Smale et al., 2019). Additionally, a decrease in the density of marine algae forests and coral bleaching (Wernberg et al., 2016; Smale et al., 2019) have also been reported.

The frequency, duration and intensity of these extreme phenomena affecting ocean systems have been increasing worryingly in recent decades (Lima and Wethey, 2012; Oliver et al., 2018; Frölicher et al., 2018; Plecha and Soares, 2020; Simon et al., 2022 and many others). As a result of global and regional warming heavily influenced by anthropogenic factors, the intensity and annual number of MHWs will continue to accelerate globally (Oliver et al., 2019; Plecha et al., 2021). Conversely, as oceans warm, MCSs are diminishing (Schlegel et al., 2021; Simon et al., 2022) and are expected to continue fading in future climate conditions (Yao et al., 2022). However, these evolutions are not uniform regionally and it remains unknown if coastal areas follow the open-ocean trends.

This paper focuses on the coastal and regional Northeast Atlantic and three subregions (English Channel, Bay of Brest and Bay of Biscay) as these zones are important for socio-economic activities (e.g. fishery; Guo et al., 2022) and have contrasted dynamical environment. Plecha et al. (2021) studied MHWs annual features in the whole North Atlantic using low-resolution satellite data at 1° × 1° over the period 1971-2000. They show that in the Bay of Biscay, the mean frequency is about 12 events per year and is characterized by ~ 12 days of mean duration and 0.4 ºC of mean intensity. Marin et al. (2021) did a global analysis of MHWs in coastal areas over the period 1992–2016 based on a satellite multi-product at a resolution from 0.25 × 0.25 up to 0.05x0.05. They found that in the Bay of Biscay and English Channel from 1992–2016, MHWs occurred on average 3 times per year lasting about 20 days with a mean intensity of 1.5°C. Here we focus on these regions on the seasonal features, such as summer MHWs and winter MCSs with a satellite product at 0.25x0.25.

Long-term ocean warming is an important driver of the increase of MHWs (Frölicher et al., 2018) and the diminishing of MCSs (Schlegel et al., 2021; Wang et al., 2022) but does not explain shorter variabilities of these events, or justify their interannual variability. These marine extreme events are also driven by other local and remote processes acting across a large range of spatial and temporal scales (Holbrook et al., 2019; Schlegel et al., 2021). Modes of atmospheric circulation variability can induce anomalous sea surface temperature (SST) through modification of air-sea heat fluxes and/or displacement due to ocean current advection (Deser et al., 2010) which for extreme cases, can lead to MHWs or MCS.

Interannual summer atmospheric variability in the North Atlantic-European sector has been shown to be predominantly led by the summer North Atlantic Oscillation (SNAO) pattern. The SNAO is identified as strong high-pressure anomalies dominating Northern Europe and weaker low-pressure over Greenland and the Iberian Peninsula which explains about 20% of the variance using sea-level pressure (Hurrell et al., 2003). The SNAO is recognized as a more northerly location and smaller spatial scale than the winter NAO pattern. During the positive phase of the SNAO, Northern Europe experiences drier, warmer and reduced cloudiness conditions, and the Bay of Biscay, the English Channel, and the North and Baltic Seas undergo warmer SST (Folland et al., 2009). The East Atlantic (EA) pattern is also identified as a dominant mode of North Atlantic atmospheric variability (Barnston and Livezey, 1987), which is particularly important for the northwest Iberian Peninsula climate in all seasons (Lorenzo et al., 2008). It is a North–South dipole that spans the entire North Atlantic Ocean, with centers southeastward to the NAO pattern (winter and summer).

Although there is strong evidence of the influence of large-scale features, no consensus exists on atmospheric patterns associated with summer MHWs in the Bay of Biscay and the English Channel. On one side, Holbrook et al. (2019) identify the Bay of Biscay as a region for which there is a significant increase in annual MHWs days during a positive phase of the NAO, based on a linearly detrended SST with satellite data and NAO index. On the other side, Izquierdo et al. (2022a) suggest, based on the analysis of two *in situ* buoys in the coastal south of the Bay of Biscay, that the incidence, duration, and intensity of spring-summer MHWs is higher during the positive phase of the EA. However, for each of these two studies, only one climate index out of the numerous modes of summer atmospheric variability in the North Atlantic-Europe sector was considered.

MCSs have also been reported to occur as a response to atmospheric forcing through anomalous winds and air-sea heat fluxes, especially in coastal regions where cold air outbreaks over shallow water can cause rapid chilling of water (Crisp, 1964; Schlegel et al., 2021). But to the best of our knowledge, no study has been published focusing on the connection between MCSs and atmospheric circulation in the Bay of Biscay and the English Channel.

At a more regional scale, Guinaldo et al. (2023) linked the 2022 MHW off France to above-average solar radiation, below-average cloud coverage and negative wind speed anomalies showing also the importance of hydrodynamic conditions such as the tide that allows turbulent vertical mixing. This explains why the Mediterranean sea with weak tidal ranges presents a more pronounced response to MHWs (Darmaraki et al., 2019; Simon et al., 2022). Other studies have been carried out in terms of processes and detection of MHWs in the Bay of Biscay but only along the Spanish Cantabrian coast. Namely, Izquierdo et al. (2022b), found a steady increase in SST from 1998 to 2019, which was reflected in MHWs occurrence and consequent match-up to report population shifts in coastal macroalgae. In a second study, Izquierdo et al. (2022a) compared MHWs with satellite data and found a 6-fold increase in their incidences in the last four decades with half of this increase related to climate change.

Several studies focus on the impact of MHWs or MCSs on biological systems, covering the areas of the Bay of Biscay, the English Channel or the Spanish Cantabrian coast, reaching as far back as the 60s of the XXth century. These studies analyzed the atmospheric cold-spells of the winter of 1962-1963 on the English coast and the impact on marine animal mortality such as *Pecten Maximus* (Crisp, 1964) or migration of species such as flounder (Sims et al., 2004). In the English Channel, Gomez and Souissi (2008) made the link between the MCS of 2005 and the absence of the spring bloom of *Phaeocystis*. A delay in the initiation of the phytoplankton bloom caused by the presence of MCS at the end of winter in the Bay of Brest and in the Bay of Vilaine (in the Northern part of the Bay of Biscay) is observed by Poppeschi et al. (2022). The impact of MHWs on biology is even more studied than the cold counterpart. Gomez and Souissi (2008) show the link between the heatwave of 2003 in the English Channel and the abundance of dinoflagellates. Joint and Smale (2017) demonstrate a link between MHWs and microbial activity assemblage in the English Channel which controls biogeochemical cycles in the ocean. The MHW of 2018 in the English Channel is present in the literature for its mortality mass impact on mussels (Seuront et al., 2019), its link to fucoids (Mieszkowska et al., 2020) or harmful phytoplankton blooms (Brown et al., 2022). Predictions at the atmospheric scale point to an increase in the future of heatwaves in the Bay of Biscay (Chust et al., 2011) and a decrease in marine fauna (Wethey and Woodin, 2022).

In this context, we aim to describe and explain the evolutions of the MHWs over summer and MCSs over winter activity in the Northeast Atlantic and to investigate the regional variability in three subregions: the English Channel, the Bay of Brest and the Bay of Biscay. The analysis will rely on both *in situ* and satellite data to address MHWs and MCSs activity, aiming to evaluate the impact of such events in coastal regions and in the open ocean. This approach will allow us to evaluate the potential use of *in situ* measurements to detect, characterize and understand such extreme events. In the last section of this paper, we focus on the influence of the interannual atmospheric mode of variability involved in the occurrence of MHWs and MCSs in the Northeast Atlantic by finding the atmospheric circulation occurring in phase with most of the strongest events.

2. Material and methods

2.1 Satellite and reanalysis data

The global SST data used in this study results from a combination of different observational platforms, including satellites, ships, buoys and Argo floats, provided by the National Oceanic and Atmospheric Administration (hereafter OISST; Reynolds et al., 2007; Huang et al., 2020). The satellite products have a daily temporal coverage for the 1982-2022 period and are interpolated to a regular global grid of 1/4º spatial resolution. Monthly geopotential height at 500 hPa (Z500), surface net short-wave radiation flux, surface net long-wave radiation flux, surface sensible heat flux and latent radiation heat flux data were obtained from the European Center for Medium-Range Weather Forecasts (ECMWF) reanalysis data ERA5 at a spatial resolution of 0.25°× 0.25° (Hersbach et al., 2019).

2.2 Buoy data

The *in situ* SST data are from autonomous coastal buoys that take continuous high-frequency measurements from 10 minutes to 1 hour (Figure 1, left panel). These buoys are from different European organizations, detailed below and in Table S1, covering the coastal areas of the English Channel, the Bay of Brest and the Bay of Biscay.

The National Observation Infrastructure network (COAST-HF, www.coast-hf.fr) operates 14 buoys taking measurements of several physical and biogeochemical data all around French coasts. Among them, 7 buoys are used here and are located in the English Channel - CARNot (https://doi.org/10.17882/39754), SMILe (https://doi.org/10.17882/53689) and ASTAn; in the Bay of Brest - IROIse (https://doi.org/10.17882/74004) and SMARt (https://doi.org/10.17882/86020) and in the Bay of Biscay - MOLIt (https://doi.org/10.17882/46529) and ARCAchon. The Met Office (www.metoffice.gov.uk) manages several buoys in each facade of England and also at offshore sites. The buoys used here are located in the English Channel, on the South coast of England, SEVEn Stones; CHANnel and GREENwich. The Western Channel Observatory (WCO, www.westernchannelobservatory.org.uk), situated within the western English Channel operates two oceanographic moorings. The station L4_Q located near the city of Plymouth, approximately 7 km offshore is used here. Puertos del Estado (www.puertos.es) operated two buoys along the Spanish coast: BILBao and GIJOn located in the Cantabrian Sea, both of them are used here.

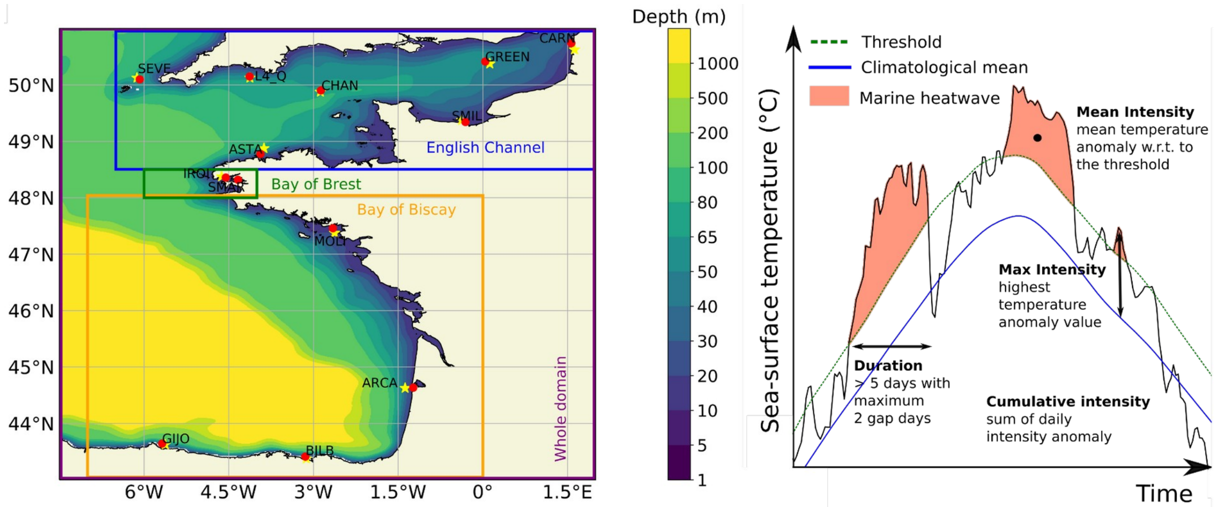

Figure 1: (Left) Map of the study area including the whole domain/Northeast Atlantic (purple box) as well as the three subregions which are the English Channel (blue box), the Bay of Brest (green box) and the Bay of Biscay (orange box). The buoys are represented by red dots and the closest satellite points are represented by yellow stars. (Right) Schematic of MHW detection and properties as defined by Hobday et al. (2016).

2.3 Detection of MHWs and MCS

To detect marine temperature extreme anomalies, we use the definition of Hobday et al. (2016). First, a climatology over 40 years, from 1982 to 2022, is calculated from the satellite product. Then, we apply the 90th percentile on summers (JJAS) for MHW and the 10th on winters (DJFM) for MCS. Finally, a MHW (MCS) is detected if values are above (below) the threshold for at least 5 days. For *in situ* data, the same detection method is applied considering the climatology calculated from the satellite product. Only seasons (summer or winter) with more than 80% of available data are analyzed.

To characterize MHW and MCS, we analyze parameters such as the number of events, the duration, the spatial extent and the cumulative intensity, defined as in Hobday et al. (2016) (Figure 1, right panel). We also explore an integrated indicator of these different parameters characterizing the marine temperature extreme events (MHWs and MCS), called activity and defined by Simon et al. (2022). This indicator estimates for each grid point the cumulative combination of the mean intensity, the duration and the affected area of each extreme event within a selective time range (for example JJAS). This activity index accounts explicitly for the area, as in most SST products a grid cell area differs from one latitude to another and marine thermal events can expand over large areas. The activity is calculated for each grid point. It sums the product of the mean intensity, duration within the selected time range, and area of each detected event occurring within the selected time range. The activity is written as follows:

$$Activity = \sum_{EE \in Time\,Range} mean\,intensity_{EE} \cdot duration_{EE \cap Time\,Range} \cdot area_{EE}$$

Where EE $\in$ time range, denotes the extreme event (EE) that occurs within the selected time range; the mean intensity of EE (in ºC) is the mean temperature anomaly with respect to the threshold of the event; duration EE $\cap$ time range (in days) is the duration of the event that remains within the considered time range, and $area_{EE}$ (in km^2) is the area affected by the discrete event within a predefined domain. Time series involving the activity metric for a domain are calculated as the mean of every grid cell considered. The activity for each station is computed in °C.days without considering the area influenced by the events as it can not be estimated from single localized stations.

This method of detection and characterization of marine thermal extreme events is performed over the whole domain of this study, referred to as the Northeast Atlantic (8° W to 2° E - 43° N to 51° N) and at each station where *in situ* observations are available. As illustrated in Figure 1, three different subregions will be analyzed in detail, namely (i) the English Channel (6.5° W to 2° E - 48.5° N to 51° N), (ii) the Bay of Brest (6° W to 4° W - 48° N to 48.5° N) and (iii) the Bay of Biscay (7° W to 0° W - 43° N to 48° N). This will allow us to explore these regions separately and highlight regional patterns. Those three subregions can be associated with three contrasted hydrodynamical regimes: macrotidal (English Channel), semi-enclosed bay (Bay of Brest), mesotidal (Bay of Biscay; Charria et al., 2013).

3. Results

3.1 Evolution of marine heatwave activity

3.1.1. An integrated regional view

MHWs were detected over the Northeast Atlantic. The activity index (Figure 2a) highlights two main periods in the MHWs dynamics. Before 2003, MHWs activity remained moderate to weak with activity generally lower than 5 °C.days.10^3 km^2 corresponding to 1.2 mean occurrences per summer with a mean duration limited to 8 days (Figure 3). Only the summer of 1989 displayed strong MHWs activity (exceeding 10 ºC.days.10^3 km^2) before 2000. From 2003 onward, the activity increased over 30 ºC.days.10^3 km^2 for summers 2018 and 2022 associated with more than 2.5 mean occurrences lasting around 20 days. The mean intensity remains quasi-steady during the whole period. The interannual variability and trend of the summer MHWs activity for the whole domain is similar to the one obtained for the average activity of the 13 grid cells closest to the buoy locations (black line of Figure 2), suggesting that at first order of magnitude, coastal and open ocean follow the same evolution.

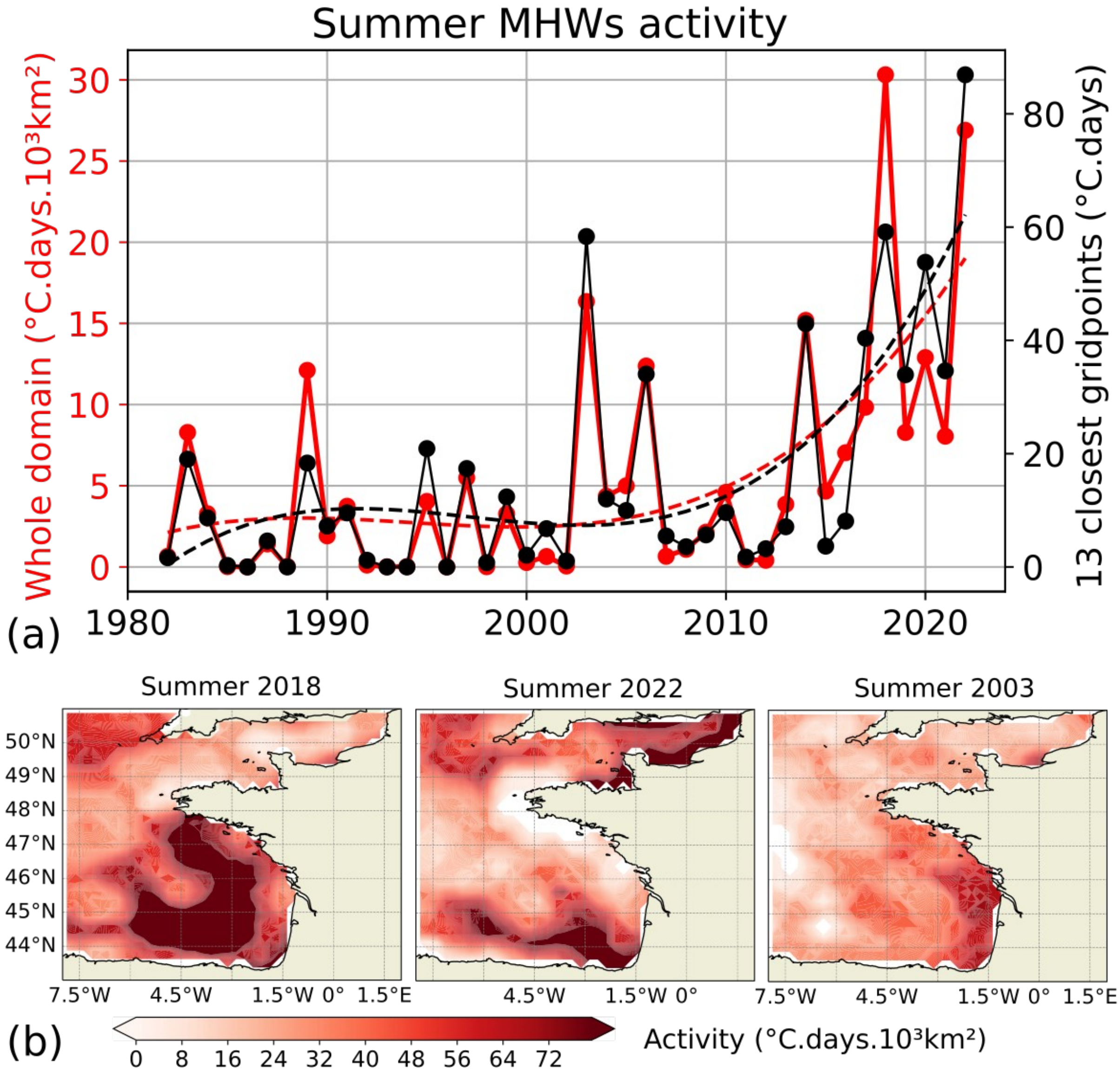

Figure 2: (a) Times series of summer (JJAS) MHWs mean activity in the Northeast Atlantic from the satellite product (red curves) and for the average of the 13 grid cells closest to the buoys from the satellite product (black curves)**.** Dash lines represent the regression of a third-order polynomial of the solid line with the same color. (b) Summer (JJAS) activity (first row; in ºC.days.10^3 km²) for the top 3 summers in terms of activity in the Northeast Atlantic (from left to right).

The three most active summers are 2018, 2022 and 2003 (Figure 2a). During 2018 (Figure 2b), maximum activity is located in the Bay of Biscay over the outer continental shelf and the continental slope from the southern part of the Biscay. These events are also extending to the North until the South of Brittany and is limited by the Ushant tidal front (Le Boyer et al., 2009; Müller et al., 2010) developed during summer. Regions of minimum activity during 2018 are West of French Brittany in the Ushant front region where tides are efficiently vertically mixing the water column. Similarly, the activity remains weak in the English Channel, as it is a macrotidal region. In terms of duration, longer events are observed in the Southern part of the Bay of Biscay exceeding 30 days (Figure S1). The 2022 summer is the second most active year for the whole domain, with over 25 °C.days.10^3 km², and also the strongest in terms of marine activity over coastal regions as shown by the maximum value of the average activity near the 13 buoys considered (Figure 2a). Spatially, the English Channel and the North of Spain record the strongest MHWs activity while the French Brittany coast has no occurrence over this year (Figure 2b). In the English Channel, the mean duration of the summer 2022 events was around 35 days (Figure S2) with localized events lasting more than 50 days (Figure S1). In Northern Spain, the duration of the events was around 20 days, however, they occurred very frequently over the summer with strong mean MHWs intensities of around 2 ºC (Figure S1). In 2003 (Figure 2c), the MHWs activity spatial distribution was different than in 2018 and 2022. The activity is larger over the inner continental shelf along Western French coasts in the Bay of Biscay. This region is under the influence of main river plumes along this coast (Adour, Gironde and Loire rivers). During this year, river discharge could have induced stratification (inducing faster warming of the surface mixed layer in regions of freshwater influence; Oh et al., 2023) and warmer waters from rivers suggest that observed MHWs were sustained by an atmospheric event more centered over lands. During this summer, the number of events is larger in the Western English Channel but shorter and less intense than in the Bay of Biscay. These top three active summers highlight the interannual spatial variability of MHWs activity. The detailed mean features (number of events, duration and mean intensity) of summer MHWs over the period 1982-2022 in the Northeast Atlantic, English Channel, Bay of Brest and Bay of Biscay are documented in Table S2.

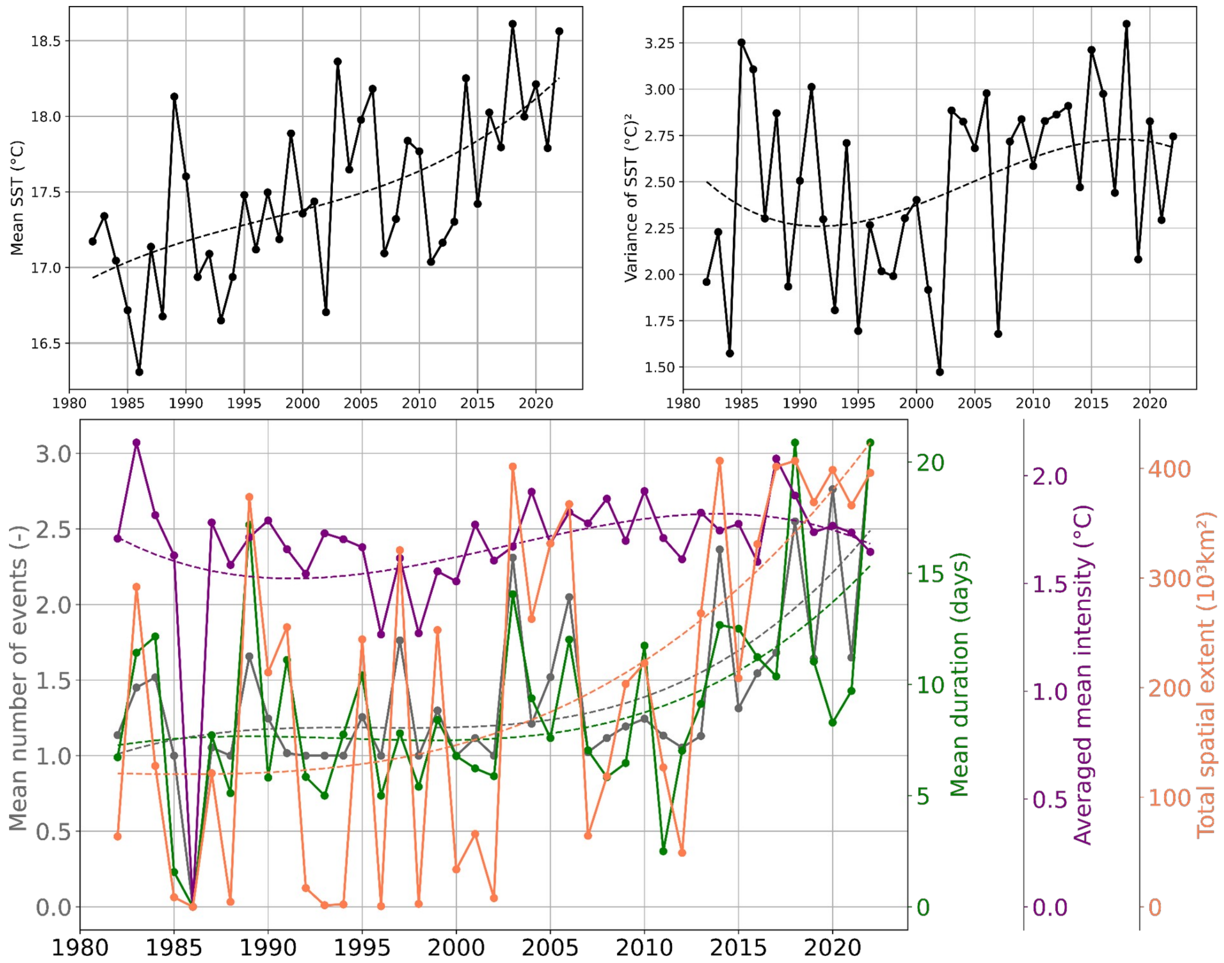

Figure 3: Time series of the mean (upper-left) and variance (upper-right) of SST (black curve) of summers (JJAS) over the Northeast Atlantic for the period 1982-2022. The SST variance is calculated for each year over the respective domain and measures the spread of the spatial distribution. (Bottom) Mean properties of summer (JJAS) MHWs in the Northeast Atlantic. The mean number of events (grey curve) is the number of events within the summer averaged

over the domain (without considering cells with zero event). Mean duration (green curve) is the average duration of every event within the summer and domain. Averaged mean intensity (purple curve) is the average of the mean intensity of every event within the period and domain. Total spatial extent (orange curve) is the sum of each grid cell area where one or more events occur. If more than one MHWs occurs on the same cell, only one grid cell area is taken into account. Dash lines represent the regression of a third-order polynomial of the solid line with the same color.

The mean SST has been increasing over the 40 years with an approximately linear trend, showing a mean warming of nearly 1.5 ºC for the whole domain since 1982 (Figure 3). Regionally, it is observed that the increase in the mean SST is almost yearly constant for the Bay of Biscay region, and quadratic for the English Channel and Bay of Brest, where a plateau is observed around 1995-2010 (Figure S2).

The SST variance is calculated for each year over the respective domain and measures the spread of the spatial distribution. Over the Northeast Atlantic, during 1985-2002 and the 5 most recent years are characterized by a decline in the SST variance, while around 1992-2017 an increase in the SST variance is observed. This interannual trend is similar to the ones observed for the events' intensity, with the exception of the English Channel, showing a direct relationship between the SST variance and the mean intensity of the MHWs events. In the English Channel, Bay of Brest and Bay of Biscay, the mean SST is warming and the variance is increasing. This estimation points that they both contribute to the changes in the respective MHWs activity (Figure S2).

Contributing to this recent increase in the Northeast Atlantic is primarily the sharp trend of the events' spatial extent (~180 to 400 °C.days.10^3 km^2), followed by the rise of the number of events (1.2 to 2.5) and also their duration (7 to 15 days; Figure 3). One should note that, for the same number of events, the events' spatial extent can differ depending on their spatial repartition, as in the events' spatial extent only one grid cell area is taken into account when more than one event occurs on the same grid. Furthermore, over the most recent years the mean number of events, their mean duration and total spatial extent reached the maximum recorded values. Since 2017, the total spatial extent over the Northeast Atlantic has recorded consecutive high values, exceeding 360.10^3 km^2. The summers of 2018, 2020 and 2022 recorded on average more than 2.5 events for almost all subregions, with events lasting on average more than 20 days in 2018 (Bay of Biscay) and 2022 (English Channel; Figure S2). Among the three studied subregions, the English Channel is the region experiencing the strongest increase in summer MHWs activity over the last four decades (see trend in Figure S3). The longest mean duration is seen in the English Channel (35 days in summer 2022), the highest mean number of events occurred in the Bay of Brest (2.7 in summer 2020) and the highest mean intensity is present in the Bay of Biscay (2.2 ºC in 2017; Figure S2).

3.1.2. Coastal MHWs activity

The spatial heterogeneity of the MHWs occurrence and activity can influence the impact of MHWs along the coastline. We then explore MHWs activity detected along the coast from *in situ* observations compared with remotely sensed observations. Figure 4 shows the activity detected for the whole Northeast Atlantic domain and in the three subregions where long-term *in situ* observations exist. To compare *in situ* and satellite data, for each station, time series based on satellite data consider only years where in situ data exists (see Table S1 for the starting date) and exceeds 80% of available data for the considered season. Linked with the whole domain activity (Figure 4a), we observe an increase in the MHWs activity in the three subregions (Figure 4b, c, d). Similar evolutions are observed when the satellite product or coastal buoys are considered. In the Bay of Brest, we also observe a similar increase but with larger activity in *in situ* observation as the intensity of extreme is underestimated by the satellite in this semi-enclosed bay. The use of *in situ* observation is limiting the length of the analyzed time series. However, we can observe larger activity in recent years from both datasets. For most cases, similar most active years are detected with *in situ* observations and satellite data.

Considering coastal stations over the observed periods, we see a more pronounced increase in MHWs activity from 2010. The English Channel and the Bay of Biscay *in situ* stations highlight the year 2022 as the most active year exceeding 140 °C.days. In the Bay of Brest, the impact of the 2022 MHWs is less pronounced, in agreement with satellite observation (Figure 2b) due to tidally driven vertical mixing.

When we compare MHWs activity estimated from *in situ* stations and satellite product, values are generally larger from *in situ* stations. Those differences are explained by the underestimation of extreme temperatures in coastal regions in remotely sensed products.

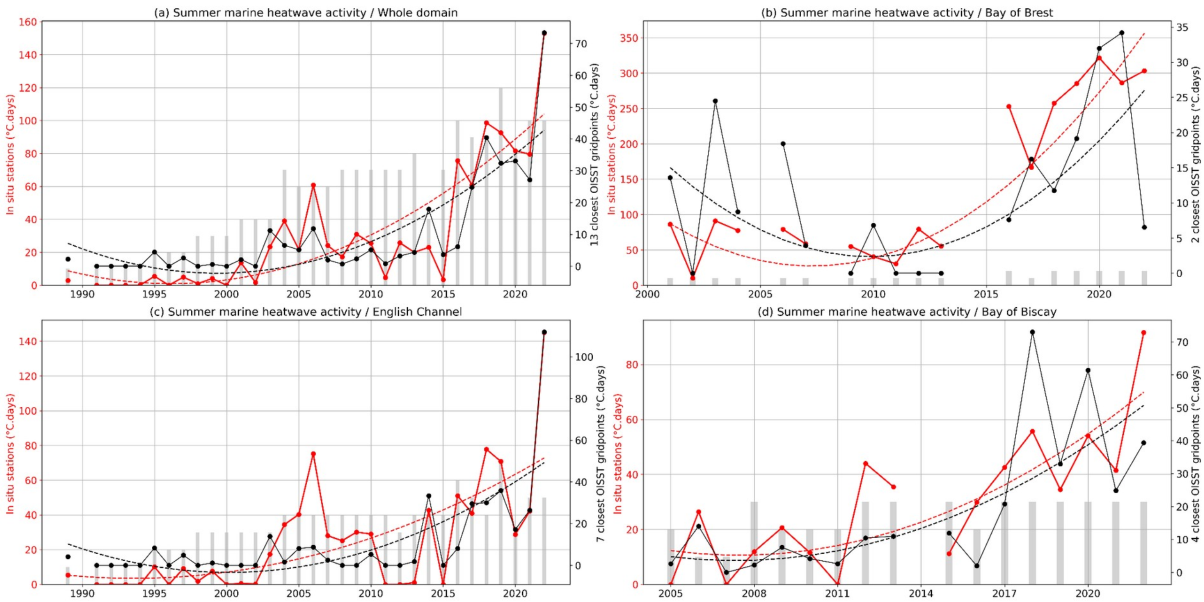

Figure 4: Time series of summer (JJAS) MHWs mean activity (a) in the whole domain (Northeast Atlantic) and in three subregions: (b) Bay of Brest, (c) the English Channel, and (d) Bay of Biscay. The red curve represents the activity based on *in situ* observations. The black curve represents the activity based on satellite dataset for the closest non-masked points with *in situ* stations when *in situ* data exists. Dash lines represent the regression of a third-order polynomial of the solid line with the same color. Grey bars are proportional to the number of considered *in situ* time series. MHWs activity from *in situ* time series with less than 80% of observation during the analyzed season is not computed.

3.2 Evolution of marine cold-spell activity

3.2.1 An integrated regional view

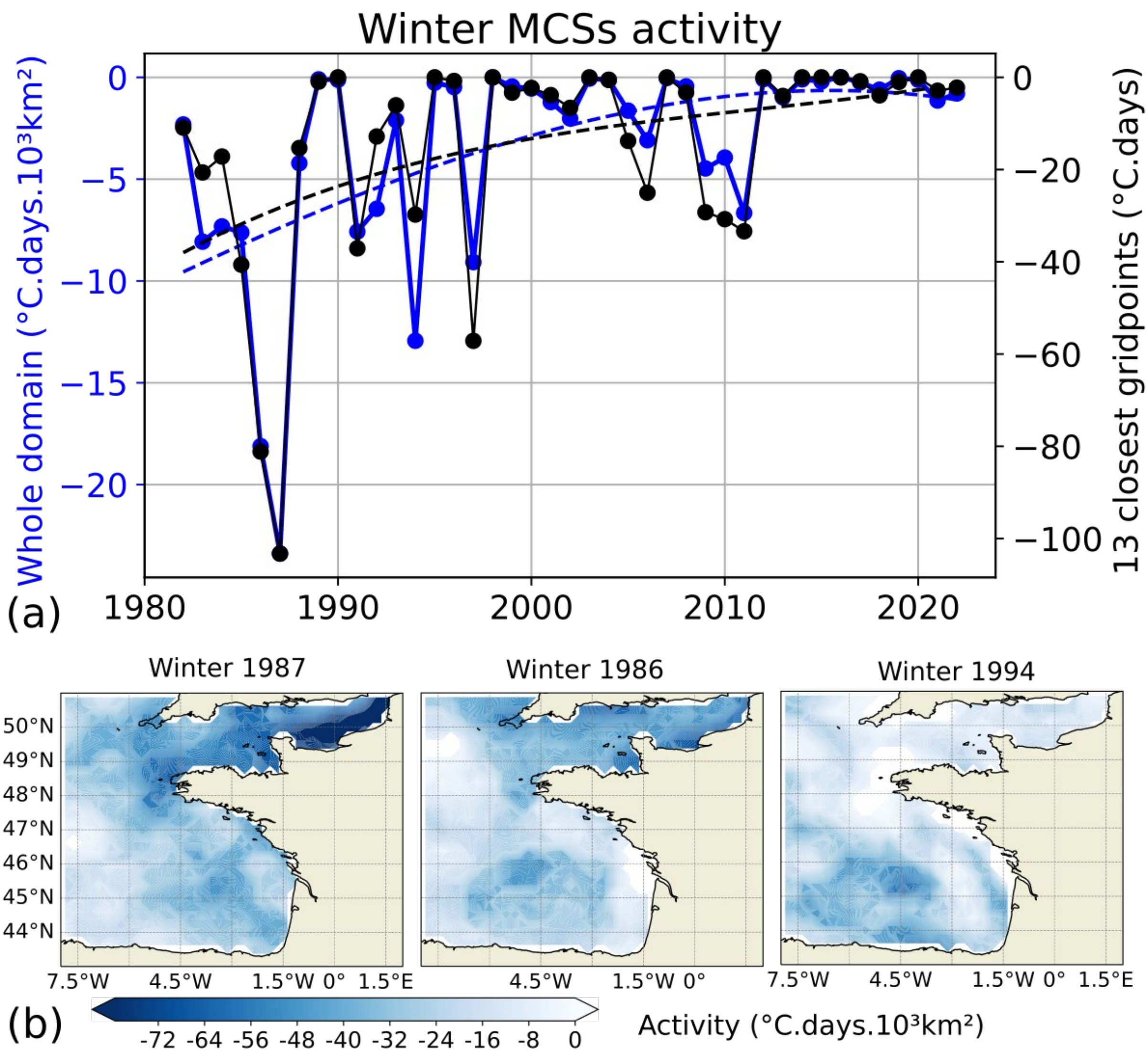

Figure 5: Same as Figure 2 but for MCSs in winter (DJFM).

Figure 5 depicts winter MCSs evolution for the whole domain over the last four decades (1982-2022). MCSs activities decrease linearly during the first half of the period, showing almost no occurrence after 2000 with the exception of 2006 and 2009 to 2011. A similar evolution is seen by considering the average of the 13 grid points closest to each *in situ* station.

The three most active MCSs occur in winter 1987 (-24 °C.days.10^3.km^2), 1986 (-18 °C.days.10.km^2) and 1994 (-13 °C.days.10^3.km^2). In the two coldest winters, MCSs were dominant in the English Channel, especially off the Northern French Coast in winter 1987. These two winters are characterized by long (~ 50 days) and intense (~ -2.5 ºC anomalous SST) and few events (~ 1 event; Figure S4). This region is subject to high turbulent mixing generated by the tidal current, which could favor cold conditions. By contrast to these two winters (1987 and 1986), winter 1994 featured strong MCSs activity in the center of the Bay of Biscay, due to numerous (~ 5 events) but moderate intensity (~ -1.3 ºC) and relatively short (20 days) events. The three winters 2009-2011 present very localized extreme cold conditions along the coastal Armorican Shelf, and additionally in the English Channel for 2011 (not shown). The detailed mean features (number of events, duration and mean intensity) of winter

MCSs over the period 1982-2022 in the Northeast Atlantic, English Channel, Bay of Brest and Bay of Biscay are documented in Table S3.

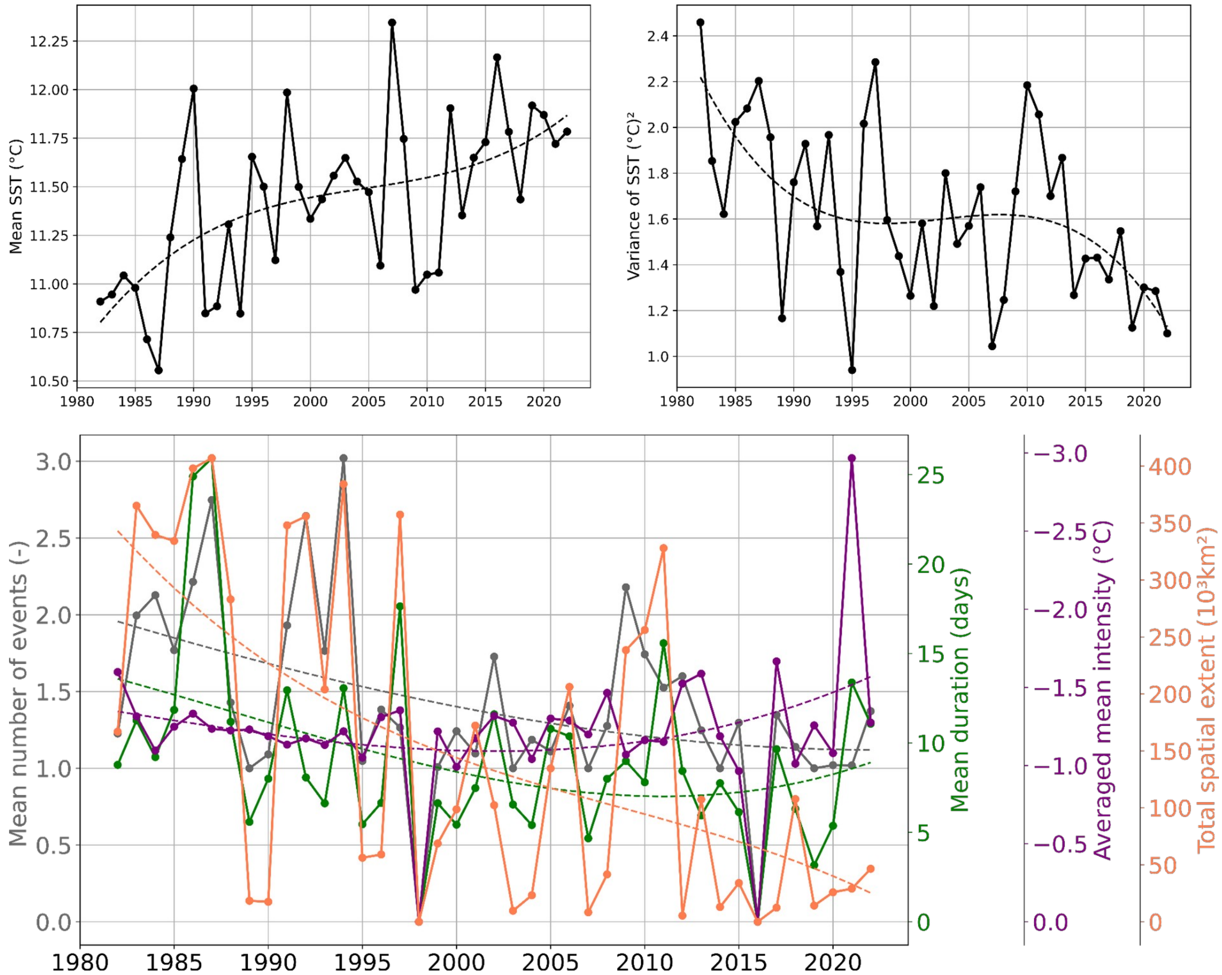

Figure 6: Same as Figure 3 but in winter (DJFM) and MCSs (blue curve)

The mean and variance evolution of SST, as well as the mean evolution of MCSs properties (occurrence, duration, mean intensity and spatial extent) are presented over the whole domain (Figure 6) and separately for the English Channel, the Bay of Brest and the Bay of Biscay (Figure S5). Over the whole Northeast Atlantic domain, the SST mean increases and spatial dispersion (variance) decreases with both a plateau around 1995-2010, following the English Channel and the Bay of Biscay evolution. On the contrary, a steady increase in the mean SST and a nearly constant variance of SST is seen in the Bay of Brest.

The warmer winter seen over the whole domain and for the three subregions is consistent with the decrease of the extremely cold conditions, depicted by the mean MCSs activity. The decrease in the mean MCSs activity is controlled by the strong decrease in spatial extent (350 to 50 $10^3.km^2$), the moderate decrease in the number of events (2 to 1.2 events), and the small decrease in duration (13 to 9 days). The mean intensity does not show any trend (~ -1.5 ºC).

The decrease of spatial dispersion (variance) of SST over the whole domain indicates a more uniform evolution which is explained by a dominant warming trend stronger for colder areas. Indeed, the relatively cold English Channel's temperature increased by 1.5 ºC (from 9 ºC to 10.5 ºC) and the relatively warmer Bay of Biscay increased by 0.8 ºC (from 11.8 ºC to 12.6 ºC) over the 1982-2022 period. When considering individually the three subregions, localized enough to be under a similar trend, the variance also decreases (Figure S5). The decrease of variance is more pronounced for the English Channel than for the Bay of Brest and Bay of Biscay. Therefore, a first estimate shows that mean SST warming and the variance changes both contribute to the changes in MCSs activity in the English Channel, Bay of Brest and Bay of Biscay.

MCSs activity generally follows the SST evolution, albeit with small differences. Indeed, winter 1991 and 1994 have a similar mean SST (10.8 ºC) but the MCSs activity is three times higher in 1994 than in 1991, driven by a higher number of events (3 instead of 2 events with similar duration, mean intensity and spatial extent).

Even if changes in winter occur in the Bay of Brest and Bay of Biscay, more drastic changes are seen in the English Channel over the period 1982-2022 (see trend in Figure S6). In the English Channel, the trend of MCSs shows at the beginning of the period, a mean occurrence of 2 events/winter, lasting 15 days with a mean intensity of -1.5 ºC over an area of 100 10^3 km^2, followed by a sharp decline ending to no detected MCSs in the last four years (2019-2022). In the Bay of Brest over the same period, MCSs properties decrease from 1.5 events during 15 days at a mean intensity of -1.4 ºC over 11 10^3 km^2 to 0.5 events during 8 days at a mean intensity of -0.8 ºC over 0.5 10^3 km^2. Exceptional long events occurred in the winter of 1987 with a mean duration of 55 days. In the Bay of Biscay, the MCSs decline in occurrence (from 2 to 1 event), duration (from 11 to 9 days) and spatial extent (170 to 40 10^3 km^2) while the mean intensity rises from -1.3 ºC to -1.5 ºC. The increase is explained by winter 2021; without these events, the mean intensity would have been nearly constant around -1.3 ºC. Indeed, winter 2021 shows a small activity but the highest mean intensity (-3 ºC over the whole domain) which is explained by a localized event in the coastal area off South-West of France with a maximum intensity of (-5.6 ºC). Apart from a very intense and localized event in the coastal area off South-West of France in winter 2021 and a very long event in the Bay of Brest in winter 1987, severe MCSs occurred predominantly in the English Channel (winter 1987 and 1986).

3.2.2. Coastal MCSs activity

Figure 7 shows the time series of MCSs activity for *in situ* data and satellite data considering the same missing data as each *in situ* station data. Along the coasts, MCSs activity as determined by local buoys remains weaker than MHWs activity as defined using satellite data. As for the MHWs, MCSs intensity is underestimated in satellite observations but evolutions are similar. From *in situ* observations from coastal stations, two years can be highlighted due to their intense MCSs: 2006 and 2010 (Figure 7). The year 2010 is the most intense, in terms of MCSs. The mean activity is reaching -100 ºC.day in the Bay of Brest and around -60 °C.day in the Bay of Biscay and the English Channel. In 2006, the activity was also important compared with other years: around -80 °C.day in the Bay of Brest and around -50 ºC.day in the English Channel. This extreme year 2006 was also unique with a peak in MHWs activity during the summer (Figure 4). Before the year 2000, only observed in the English Channel from coastal stations, three other years reveal intense MCSs activity: 1997, 1991, 1994 (from the most intense to the less active winter) from satellite data at the closest point of *in-situ* data.

We do not detect a significant trend in the interannual evolution of MCSs activity along the coasts. For the Bay of Biscay and the Bay of Brest, it can be directly connected to the lack of observation before 2000 when the largest MCS occurs. In the English Channel, the lack of observation also explains the observed lack of trend. Indeed, only one time series was available before 1995 and this station (GREENwich) is not detecting an important MCSs activity before 2000.

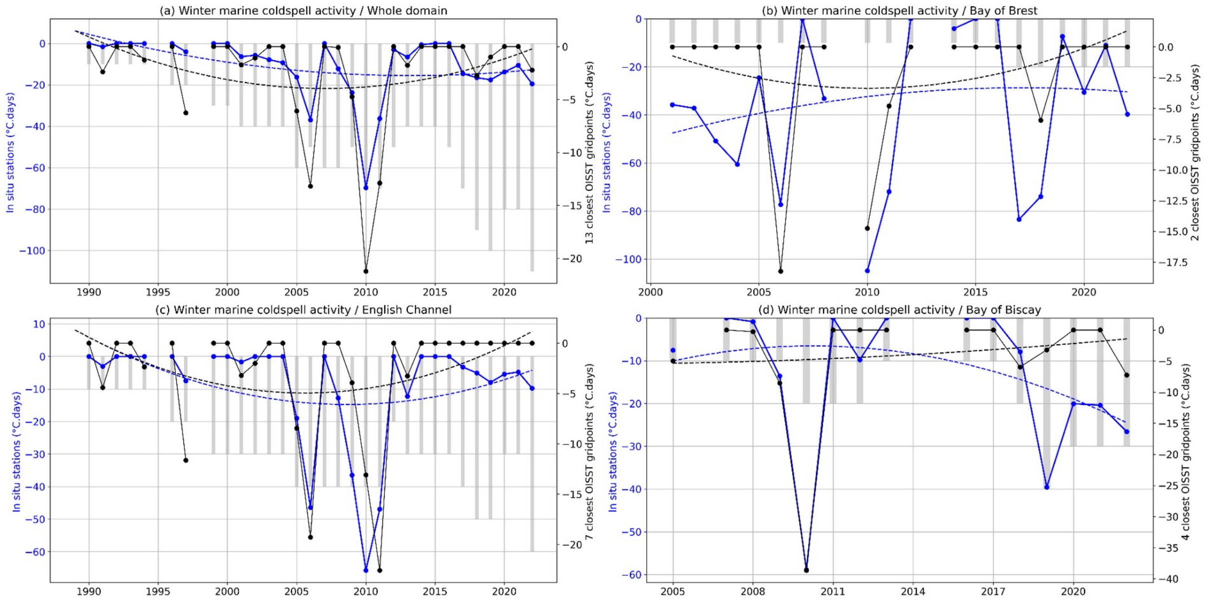

Figure 7: Same as Figure 4 but for MCSs in winter (DJFM).

3.3 Associated atmospheric patterns

Apart from the long-term trend of increasing SST, we also see high interannual variability which is potentially connected with atmospheric forcing modes (Holbrook et al. 2019; Izquierdo et al., 2022a). Figure 8 presents the atmospheric circulation in the North Atlantic associated with strong interannual MHWs in the Bay of Biscay and the English Channel. For each summer of the 1982-2022 period, MHWs total activity anomaly in the studied area box (Northeast Atlantic) with respect to the third-order long-term trend (red dotted curved in Figure 2a) was computed. This anomaly represents the detrended or interannual MHWs activity. Eight summers were identified as having high interannual activities (anomalous total activity exceeding a threshold of 4 °C.days.10^6.km², coloured marker in Figure 8 left panel). The year 2018 (23 °C.days.10^6.km²), 2003 (17 °C.days.10^6.km²) and 2006 (12 °C.days.10^6.km²) are the three strongest summers. Six out of these eight summers (all except 2018 and 2022) have an anomalous geopotential height at 500 hPa which is positive over Northern Europe (box A in Figure 8) and negative in the West of the Iberian Peninsula (box B in Figure 8). The composite of the anomalous geopotential height at 500 hPa for these six summers shows in the North Atlantic-Europe sector a positive summer NAO-like pattern, with a high over the Nordic sea and two lows over the Iberian Peninsula and Greenland. This overall result is not sensitive to small displacements of boxes (a few latitude and longitude degrees; not shown).

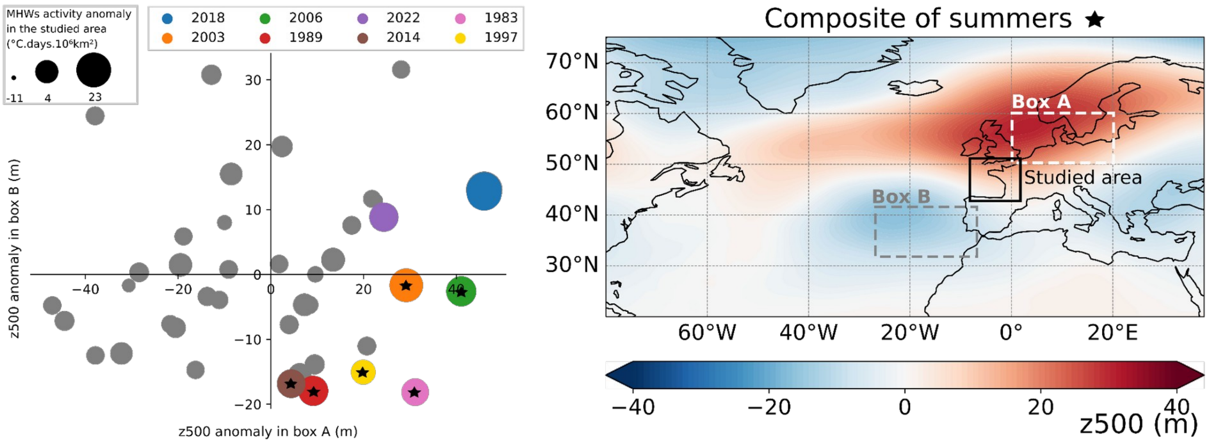

Figure 8: (Left panel) Scatter plot of anomalous summer (JJAS) geopotential height at 500 hPa (z500; in m) in box A versus the anomalous geopotential height at 500 hPa in box B with respect to the summer period 1982-2022. The size of the marker is proportional to the anomalous summer (JJAS) MHWs total activity, calculated as the sum of all grid point activity in the studied area (in °C.days.10^6.km^2) with respect to the trend (red dotted curved in Figure 2a). Markers are in color when this value exceeds 4 °C.days.10^6.km^2 and the stars are indicated when markers in color are in the lower-right “cluster” of the graph. (Right panel) Composites of summers (JJAS) marked with stars in the left panel of the anomalous geopotential height at 500 hPa (m) with respect to the summer period 1982-2022. Box A is the domain 0°E to 20°E-50 °N to 60°N and box B is the domain 33°W to 13°W - 31°N to 41°N.

Summer (JJAS) 2018 has the strongest anomalous MHWs activity in the Northeast Atlantic but, at the difference to the six next summers in the ranking of detrended MHWs activity, does not present a decrease in the geopotential height at 500 hPa in the West of Iberian Peninsula (box B). A broad high-pressure system in the North Atlantic-European sector is seen (including box A), except in the Eastern Mediterranean and up to 60°N where a low occurs (Figure S7). This response in box B for summer 2018 is primarily due to late summer (August and September) atmospheric circulation (Figure S7). These months have a minor contribution to MHWs total activity for the whole summer (JJAS; Figure S8). When considering the month of June, with 2018 MHWs peaks (Figure S8), the North Atlantic shows a positive summer NAO regime, similar to the next six summers' highest MHWs activity. This analysis demonstrates that MHWs in the Northeast Atlantic is closely associated with a high-pressure system over Northern Europe, and a low off the Iberian Peninsula, resembling the positive phase of the summer NAO. By performing this analysis with SST instead of MHWs activity, we obtain similar results, albeit with a less extended high over Northern Europe (Figure S9).

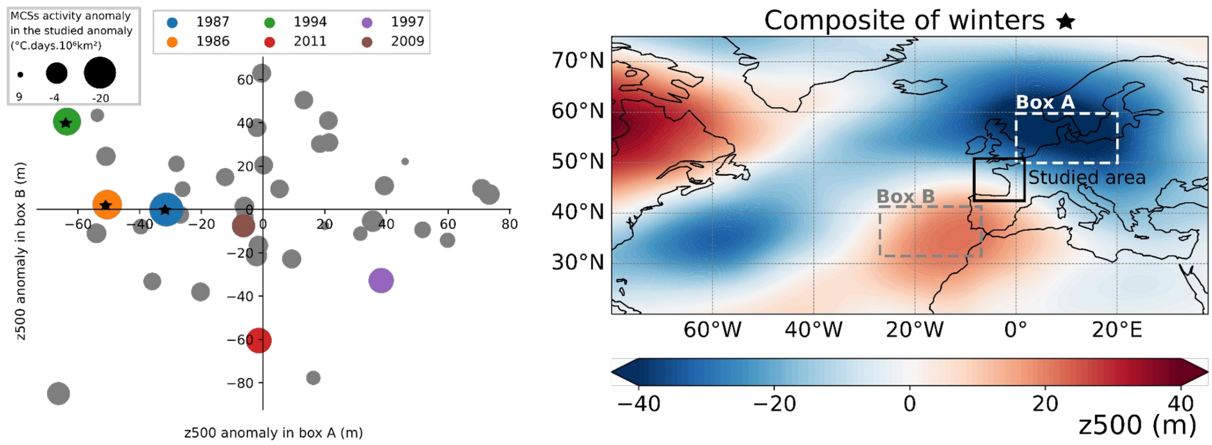

Figure 9: Same as Figure 8 but for MCSs in winter (DJFM). MCSs anomalies are calculated with respect to the third-order trend (blue dotted curved in Figure 5). Markers are in color when this value is below -4 °C.days.10^6.km^2 and stars are indicated when markers in color are in the upper-left section of the graph.

Regarding MCS, the three highest detrended MCSs activities are winter 1987 (-20 °C.days.10^6.km^2), 1986 (-13 °C.days.10^6.km^2) and 1994 (-10 °C.days.10^6.km^2; Figure 9). These three most active winters are in the same “cluster”, with an anomalous geopotential height at 500 hPa negative over Northern Europe and positive in the West of the Iberian Peninsula. Composite of the anomalous geopotential height at 500 hPa for these three winters shows in the North Atlantic-Europe sector a broad and strong low in Northern Europe, a weaker low-pressure system sitting in the Northwest Atlantic, and two highs off the Iberian Peninsula and over the Hudson Bay. This analysis suggests that extreme MCSs in the Northeast Atlantic might be closely associated with a low over Northern Europe and a high off the Iberian Peninsula. By performing this analysis with SST instead of the MCSs activity (Figure S10), the result are sparse, showing only winter 1986 as strong anomalous cold SST linked to an anomalous geopotential height at 500 hPa over Northern Europe and positive in the West of the Iberian Peninsula.

When comparing the anomalous geopotential height conditions for the most intense summer MHWs and winter MCS, we see that the geopotential height conditions are somehow opposite, although the amplitude is stronger for winter, consistent with stronger climatology (Folland et al., 2009). However, while summer MHWs are associated with a positive summer NAO, winter MCSs do not present a negative winter NAO general pattern.

To provide indications on the drivers of these events, we have considered the different components of air-sea heat flux anomalies concomitant with MHWs and MCSs. For the eight most severe interannual summer MHWs (see marker in color Figure 8) and the six most severe interannual winter MCSs (see marker in color Figure 9), the anomalous (i) short-wave radiation flux, (ii) surface net long-wave radiation flux, (iii) surface sensible heat flux and (iv) latent heat flux are depicted, respectively Figure S11 and Figure S12. The interannual (or detrended) summer MHWs are predominantly driven by high short-wave radiation flux, except for years 1983 and 1997 that only shows important positive downward latent heat flux. The other air-sea flux have a smaller contribution. The interannual winter MCSs seem to be mostly driven by high sensible heat flux and low short-wave radiation flux. This suggests that, in this region, low cloud cover is a key parameter for the generation of summer MHWs while strong winds and high cloud cover are important for the apparition of winter MCSs. Further analysis needs to be done to attribute quantitatively the contribution of each air-sea heat flux component.

4. Discussion

In the Northeast Atlantic, an increase in the MHWs activity and a decrease in MCSs activity were observed. Interannual changes confirm that general large scale trends (Oliver et al., 2018; Schlegel et al., 2021) are also observed in regions where the coastal hydrodynamics could limit the impact due to active vertical mixing processes (*e.g.* barotropic and internal tides, wind-driven mixing in shallow waters).

The most active summer MHWs analyzed over the Northeast Atlantic and in the period 1982-2022 occurred in the Bay of Biscay (2018) and the most active winter MCSs occurred in the English Channel (1987). This is consistent with Schlegel et al. (2021) who found that the maximum intensity of MHWs dominates MCSs in the Bay of Biscay, and vice versa in the English Channel. Along the coasts, the maximum of MHWs activity is detected in 2022 in the English Channel which might be related to the summer European heatwaves recorded (ECMWF, 2022; Savu, 2022; Guinaldo et al., 2023).

In the Bay of Biscay, we see a linear warming rate in summer since the beginning of the studied period. This is in accordance with DeCastro et al. (2009) which shows a steady linear warming rate since the 1970s, based on data from 1854-2006. Mean SST together with SST variance increase justify the rise of MHW. This increase of MHWs is consistent with Izquierdo et al. (2022a) who determined more precisely an equal contribution of each of these two factors for the South coast of the Bay of Biscay. This is specific to this region (as well as for the Bay of Brest and the English Channel), as for most of the other regions of the world, the mean warming and not the SST variability changes contribute to the increase in MHWs features (Alexander et al., 2018; Oliver et al., 2020). Besides, we found a positive trend for the MHWs activity parameter using both satellite data and the 4 buoys in the Bay of Biscay, and for the duration and occurrence using satellite data. The trends are quasi-similar considering only the two buoys on the South coast of the Bay of Biscay (GIJO and BILB) and the two on the West coast of the Bay of Biscay (ARCA and MOLI; not shown) and are marked by the high activity present in the more recent summers. This evolution in the occurrence and duration of MHWs were not seen in Izquierdo et al. (2022b) using two buoys in the South coastal Bay of Biscay over the period 1998-2018, which could be explained by local process or studied season (March to August).

The results from *in situ* and satellite datasets for each of the studied regions are quite in agreement, albeit the satellite underestimates the amplitude of activity for both MHWs and MCS. Conversely, Izquierdo et al. (2022a) found an overestimation of the MHWs using satellites compared to *in situ* in the coastal upwelling region South of the Bay of Biscay, which might be related to local processes. The satellite's coarse resolution mostly (i) smoothes small-scale and short events and (ii) interpolates with offshore regions, having greater thermal inertia (Marin et al., 2021) which can lead to the overestimation of the duration of events and the underestimation of the intensity. However, we show that coastal *in situ* stations distributed along the Northeast Atlantic coasts allow the detection of large-scale evolutions of MHWs and MCSs activity. Analyzed locally, they can also inform on evolutions related to local hydrodynamics.

Internal variability of winter MCSs is related to low pressure over Northern Europe and a high-pressure West of the Iberian Peninsula for three (1987, 1986 and 1994) out of the six most intense events. Among other strong interannual MCSs, winter 2011 does not present this pattern but could have been generated by a cold air outbreak brought by a ridge over Greenland (Norris et al., 2013). A relation at an interannual timescale could exist between MCSs (Figure 7, middle panel) and extreme low-salinity events (Poppeschi et al., 2021) in winter in the Bay of Brest, as, using the same *in situ* buoys (COAST-HF-Iroise from 2000-2018), two out of the four most severe low-salinity events are concomitant with MCSs (winter 2001 and 2007). These extreme events could be both influenced by intense mid-latitude depressions, but river discharges are also an important driver in this region. Unlike MHWs (Figure 2), extreme cold conditions occurred several winters in a row: three in 2009-2011 and two in 1986-1987. This might be explained by the re-emergence of cold water originating from the previous winter, as for the 2013-2016 north Atlantic cold Blob (Duchez et al., 2016a; Josey et al., 2018; Schlegel et al., 2021).

Summer 2018 presents the most active MHWs in the Northeast Atlantic for the period 1982-2022, consistent with the reported warmer SST (+1 to +3 °C above the long-term climatology) the same summer in the proximity of the United Kingdom (McCarty et al., 2019). On the continental side, this summer was also recorded as the hottest in the United Kingdom since 1884 (McCarty et al., 2019) and one of the hottest over northwestern Europe (Met Office, 2018; Météo-France, 2018). On top of the underlying warming climate forcing (Vogel et al., 2019; Yiou et al., 2020), this extreme continental warm conditions in 2018 have been previously reported as a consequence of the positive summer NAO anomalies combined with elevated SST (McCarty et al., 2019) or combined with stationary Rossby waves in synoptic anomalies (Drouard et al., 2019; Kornhuber et al., 2019). More generally, the positive phase of the summer NAO is associated with warm anomalies from the West of the United Kingdom to the Baltic (Folland et al., 2009). Our findings on the ocean side corroborate the continental counterpart as extremely warm conditions in the Bay of Biscay and the English Channel are likely associated with positive summer NAO, consistent with the result of Holbrook et al. (2019).

Depending on the region and the event, MHWs can be associated with anomalous air–sea heat fluxes which can include high short-wave, due to less cloud cover and greater insolation, high sensible heat fluxes when the surface air is warm and/or low latent heat loss from the ocean, due to weak winds (Oliver et al., 2021). In the English Channel and the Bay of Biscay, Guinaldo et al. (2023) linked the summer of 2022 sea-surface temperature to abnormally high short-wave radiation in the Bay of Biscay and English Channel. In this study, a similar conclusion is found by considering the eight most severe interannual MHWs in the Northeast Atlantic (which includes the English Channel and the Bay of Biscay, and summer of 2022). Abnormally high short-wave radiation is likely associated with reduced cloudiness and Folland et al. (2009) have found that during the positive index phase of the summer NAO, northwest Europe experiences significantly reduced cloudiness. This is consistent with our suggestion that the positive phase of the summer NAO favours the generations of summer MHWs in the Northeast Atlantic through reduced cloudiness. MCSs in the English Channel are associated with high sensible heat flux, consistent with reported MCSs often driven by strong winds in shallow waters, enabling a rapid chilling of the surface water (Crisp, 1964; Schlegel et al., 2021). We also found a possible role of weaker short-wave radiation, which might be related to increased cloud coverage.

In the future and under increasing greenhouse gas concentrations, climate models predict that the ocean surface in the Bay of Biscay and the English Channel will continue to warm (Fox-Kemper et al., 2021) and a trend toward a positive summer NAO pattern (Faranda et al., 2019). Both these effects imply the long-term likelihood of increased MHWs in the

Northeast Atlantic, but to what extent are the long-term and the interannual variability contributions remain to be shown. Also, the role of large-scale ocean circulation features, such as the Shelf Edge Current (Alheit et al., 2019) or Iberian Poleward Current (Charria et al., 2013), upper ocean preconditioning (Josey et al., 2018), and the importance of remote large-scale climate modes of variability, such as the Indian Ocean Dipole (Holbrook et al., 2019) in amplifying or suppressing MHWs occurrences in the Bay of Biscay and English Channel would need specific investigation. Along the coasts, the role of main river inflow at the land-sea continuum can also lead to specific answers on the coastal ocean to future climate evolutions.

5. Conclusions

The activity index, a combination of the properties of marine extreme events, shows a positive trend for summer MHWs in the Northeast Atlantic (since 2000 and more pronounced since 2010) and in the three subregions, the English Channel, the Bay of Brest and the Bay of Biscay for both *in situ* and satellite data. This is explained by both a mean and variance SST increase. Conversely, a decrease in MCSs activity was detected, with almost no events after 2000, more clearly with the satellite data due to the longest time series (40 years) compared with the *in situ* (20 to 30 years). These changes are fast for the three subregions, with the English Channel being the subregion with the more drastic growth.
In the Northeast Atlantic, MHWs are more frequent, longer, and extend over larger areas, while the opposite is seen for MCSs. For both MHWs and MCSs, the mean intensity shows only weak changes over the last four decades.
Moreover, we found that the satellite dataset used is in good accordance with *in situ* data in the Northeast Atlantic, except for the fact that satellites underestimate the amplitude of both hot summer and cold winter marine extreme events in the coastal areas. The implemented *in situ* stations appear as a well-designed observing system to detect the long-term evolution of MHWs and MCSs activity and to document local features related to coastal hydrodynamics.

MHWs activity is particularly high in 2018 and 2022 through two different situations. The year 2018 is characterized by a large extent of MHWs in the Bay of Biscay with long events in the South of the Bay and intense events in the Armorican Shelf. The summer of 2022 features long MHWs mainly in the English Channel. MCSs activity is the highest in 1986 and 1987 due to long and intense events in the English Channel.

Our findings show that summers with strong MHWs activity due to internal variability (after removing the trend) in Northeast Atlantic have often been associated with a ridge over the northern Europe sea and a trough West of the Iberian Peninsula; the opposite situation is seen for MCSs. In the case of MHW, the wide atmospheric pattern resembles the positive phase of the summer NAO. This preliminary analysis of air-sea heat flux suggests that in the Northeast Atlantic interannual (or detrended) summer MHWs are predominantly driven by high short-wave radiation flux and interannual winter MCSs by high sensible heat flux and low short-wave radiation. This suggests that, in this region, low cloud cover is a key parameter for the generation of summer MHWs while strong winds and high cloud cover is important for the apparition of winter MCSs. We caution that the proposed connection does not necessarily indicate causal links but these relations can provide indications of drivers.

Despite contrasted hydrodynamical regimes (meso- and macro-tidal) and circulation (shallow water under freshwater influence, shelf circulation, active sub-mesoscale), the Northeast Atlantic region displays similar changes in MHWs and MCSs activity between coastal and open ocean regions. Those changes need to be anticipated to mitigate the impacts on coastal ecosystems.

Acknowledgements

This work was partially supported by national funds through FCT (Fundação para a Ciência e a Tecnologia, Portugal) through project ROADMAP (JPIOCEANS/0001/2019). It is also funded by the regional project (Contrat Plan Etat-Region) ObsOcean/ROEC-ILICO and the regional COXTCLIM project funded by the Loire-Brittany Water Agency, the Brittany region, and Ifremer. We thank Oregan Segalen for fruitful discussions. We thank Tim Smyth for providing data from Western Channel Observatory. We acknowledge the COAST-HF (http://www.coast-hf.fr) national observing network component of the National Research Infrastructure ILICO.

Declaration of competing interest

The authors declare that they have no known competing financial interests or personal relationships that could have appeared to influence the work reported in this paper.

Authors contributions

All authors contributed to the conception and design of the study. AS performed the calculation and designed the figures involving the satellite dataset, GC and CP did so for the *in situ* dataset. All authors contributed to the discussion, writing and review of the manuscript.

References

Alexander, M. A., Scott, J. D., Friedland, K. D., Mills, K. E., Nye, J. A., Pershing, A. J., & Thomas, A. C. (2018). Projected sea surface temperatures over the 21st century: Changes in the mean, variability and extremes for large marine ecosystem regions of Northern Oceans. *Elementa: Science of the Anthropocene*, *6*.

Alheit, J., Gröger, J., Licandro, P., McQuinn, I. H., Pohlmann, T., & Tsikliras, A. C. (2019). What happened in the mid-1990s? The coupled ocean-atmosphere processes behind climate-induced ecosystem changes in the Northeast Atlantic and the Mediterranean. *Deep Sea Research Part II: Topical Studies in Oceanography*, *159*, 130-142. https://doi.org/10.1016/j.dsr2.2018.11.011

Barnston, A. G., & Livezey, R. E. (1987). Classification, seasonality and persistence of low-frequency atmospheric circulation patterns. *Monthly weather review*, *115*(6), 1083-1126. https://doi.org/10.1175/1520-0493

Brown Ross, A., Lilley, M. K. S., Shutler, J., Widdicombe, C., Rooks, P., McEvoy, A., Torres, R., Artioli, Y., Rawle, G., Homyard, J., Tyler, C. R., & Lowe, C. (2022). Harmful Algal Blooms and their impacts on shellfish mariculture follow regionally distinct patterns of water circulation in the western English Channel during the 2018 heatwave. *Harmful Algae*, *111*(December 2021), 102166. https://doi.org/10.1016/j.hal.2021.102166

Charria, G., Lazure, P., Le Cann, B., Serpette, A., Reverdin, G., Louazel, S., Batifoulier, F., Dumas, F., Pichon, A., & Morel, Y. (2013). Surface layer circulation derived from Lagrangian drifters in the Bay of Biscay, *Journal of Marine Systems*, 109, 60–76. https://doi.org/10.1016/j.jmarsys.2011.09.015

Chust, G., Borja, Á., Caballero, A., Irigoien, X., Sáenz, J., Moncho, R., Marcos, M., Liria, P., Hidalgo, J., Valle, M., & Valencia, V. (2011). Climate change impacts on coastal and pelagic environments in the southeastern Bay of Biscay. *Climate Research*, *48*(2–3), 307–332. https://doi.org/10.3354/cr00914

Crisp, D. J. (1964). The Effects of the Severe Winter of 1962-63 on Marine Life in Britain. Journal of Animal Ecology, 33(1), 165-210, https://www.jstor.org/stable/2355

Darmaraki, S., Somot, S., Sevault, F., & Nabat, P. (2019). Past Variability of Mediterranean Sea Marine Heatwaves. *Geophysical Research Letters*, *46*(16), 9813–9823. https://doi.org/10.1029/2019GL082933

DeCastro, M., Gómez-Gesteira, M., Alvarez, I., & Gesteira, J. L. G. (2009). Present warming within the context of cooling–warming cycles observed since 1854 in the Bay of Biscay. *Continental Shelf Research*, *29*(8), 1053-1059. https://doi.org/10.1016/j.csr.2008.11.016

Deser, C., Alexander, M. A., Xie, S. P., & Phillips, A. S. (2010). Sea surface temperature variability: Patterns and mechanisms. *Annual review of marine science*, *2*, 115-143.

Drouard, M., Kornhuber, K., & Woollings, T. (2019). Disentangling dynamic contributions to summer 2018 anomalous weather over Europe. *Geophysical Research Letters*, *46*(21), 12537-12546. https://doi.org/10.1029/2019GL084601

ECMWF (2022). Update on European heatwave of July 2022 (available at: www.ecmwf.int/en/about/media-centre/focus/2022/update-european-heatwave-july-2022)

Faranda, D., Alvarez-Castro, M. C., Messori, G., Rodrigues, D., & Yiou, P. (2019). The hammam effect or how a warm ocean enhances large scale atmospheric predictability. *Nature communications*, *10*(1), 1-7. https://doi.org/10.1038/s41467-019-09305-8

Folland, C. K., Knight, J., Linderholm, H. W., Fereday, D., Ineson, S., & Hurrell, J. W. (2009). The summer North Atlantic Oscillation: past, present, and future. *Journal of Climate*, *22*(5), 1082-1103.

Fox-Kemper, B., H.T. Hewitt, C. Xiao, G. Aðalgeirsdóttir, S.S. Drijfhout, T.L. Edwards, N.R. Golledge, M. Hemer, R.E. Kopp, G. Krinner, A. Mix, D. Notz, S. Nowicki, I.S. Nurhati, L. Ruiz, J.-B. Sallée, A.B.A. Slangen, & Y. Yu, (2021). Ocean, Cryosphere and Sea Level Change. In *Climate Change 2021: The Physical Science Basis. Contribution of Working Group I to the Sixth Assessment Report of the Intergovernmental Panel on Climate Change* [Masson-Delmotte, V., P. Zhai, A. Pirani, S.L. Connors, C. Péan, S. Berger, N. Caud, Y. Chen, L. Goldfarb, M.I. Gomis, M. Huang, K. Leitzell, E. Lonnoy, J.B.R. Matthews, T.K. Maycock, T. Waterfield, O. Yelekçi, R. Yu, and B. Zhou (eds.)]. Cambridge University Press, Cambridge, United Kingdom and New York, NY, USA, 1211–1362. https://doi.org/ 10.1017/9781009157896.011

Frölicher, T. L., Fischer, E. M., & Gruber, N. (2018). Marine heatwaves under global warming. *Nature*, *560*(7718), 360-364. https://doi.org/10.1038/s41586-018-0383-9

Frölicher, T., & Laufkötter, C. (2018). Emerging risks from marine heat waves. *Nature Communications*, 9(1), 2015–2018. https://doi.org/10.1038/s41467-018-03163-6

Gómez, F., & Souissi, S. (2008). The impact of the 2003 summer heat wave and the 2005 late cold wave on the phytoplankton in the north-eastern English Channel. *Comptes Rendus - Biologies*, *331*(9), 678–685. https://doi.org/10.1016/j.crvi.2008.06.005

Guinaldo, T., Voldoire, A., Waldman, R., Saux Picart, S., & Roquet, H. (2023). Response of the sea surface temperature to heatwaves during the France 2022 meteorological summer. *Ocean Science*, *19*(3), 629-647.

Guo, X., Gao, Y., Zhang, S., Wu, L., Chang, P., Cai, W., ... & Gao, H. (2022). Threat by marine heatwaves to adaptive large marine ecosystems in an eddy-resolving model. *Nature climate change*, *12*(2), 179-186.

Hersbach, H., Bell, B., Berrisford, P., Hirahara, S., Horányi, A., Muñoz-Sabater, J., ... & Thépaut, J. N. (2020). The ERA5 global reanalysis. Quarterly Journal of the Royal Meteorological Society, 146(730), 1999-2049. (Accessed on 25-05-2023)

Hobday, A. J., Alexander, L. V., Perkins, S. E., Smale, D. A., Straub, S. C., Oliver, E. C. J., Benthuysen, J. A., Burrows, M. T., Donat, M. G., Feng, M., Holbrook, N. J., Moore, P. J., Scannell, H. A., Sen Gupta, A., & Wernberg, T. (2016). A hierarchical approach to defining marine heatwaves. *Progress in Oceanography*, 141, 227–238. https://doi.org/10.1016/j.pocean.2015.12.014

Holbrook, N. J., Scannell, H. A., Sen Gupta, A., Benthuysen, J. A., Feng, M., Oliver, E. C., Alexander, L., Burrows, M., Donat, M., Hobday, A., Moore, P., Perkins-Kirkpatrick, S., Smale, D., Straub, S., & Wernberg, T. (2019). A global assessment of marine heatwaves and their drivers. *Nature Communications*, *10*(1), 1-13. https://doi.org/10.1038/s41467-019-10206-z

Huang, B., C. Liu, V. Banzon, E. Freeman, G. Graham, B. Hankins, T. Smith, and H.-M. Zhang, 2020: Improvements of the Daily Optimum Interpolation Sea Surface Temperature (DOISST) Version 2.1, *Journal of Climate*, 34, 2923-2939. https://doi.org/ 10.1175/JCLI-D-20-0166

Hurrell, J. W., Kushnir, Y., Ottersen, G., & Visbeck, M. (2003). An overview of the North Atlantic oscillation. *Geophysical Monograph-American Geophysical Union*, *134*, 1-36. https://doi.org/10.1029/134GM01

Izquierdo, P., Rico, J. M., Taboada, F. G., González-Gil, R., & Arrontes, J. (2022a). Characterization of marine heatwaves in the Cantabrian Sea, SW Bay of Biscay. *Estuarine, Coastal and Shelf Science*, *274*(June). https://doi.org/10.1016/j.ecss.2022.107923

Izquierdo, P., Taboada, F. G., González-Gil, R., Arrontes, J., & Rico, J. M. (2022b). Alongshore upwelling modulates the intensity of marine heatwaves in a temperate coastal sea. *Science of the Total Environment*, *835*(February). https://doi.org/10.1016/j.scitotenv.2022.155478

Joint, I., & Smale, D. A. (2017). Marine heatwaves and optimal temperatures for microbial assemblage activity. *FEMS Microbiology Ecology*, *93*(2), 1–9. https://doi.org/10.1093/femsec/fiw243

Josey, S.A., Hirschi, J.-M., Sinha, B., Duchez, A., Grist, J.P., Marsh, R., 2018. The recent Atlantic cold anomaly: Causes, consequences, and related phenomena. Ann. Rev. Marine Sci. 10 (1), 475–501.

Kornhuber, K., Osprey, S., Coumou, D., Petri, S., Petoukhov, V., Rahmstorf, S., & Gray, L. (2019). Extreme weather events in early summer 2018 connected by a recurrent hemispheric wave-7 pattern. *Environmental Research Letters*, *14*(5), 054002. https://doi.org/10.1088/1748-9326/ab13bf

Le Boyer, A., Cambon, G., Daniault, N., Herbette, S., Le Cann, B., Marie, L., & Morin, P. (2009). Observations of the Ushant tidal front in September 2007. Continental Shelf Research, 29(8), 1026-1037.

Lima, F. P., & Wethey, D. S. (2012). Three decades of high-resolution coastal sea surface temperatures reveal more than warming. *Nature communications*, *3*(1), 704.

Lorenzo, M. N., Taboada, J. J., & Gimeno, L. (2008). Links between circulation weather types and teleconnection patterns and their influence on precipitation patterns in Galicia (NW Spain). *International Journal of Climatology: A Journal of the Royal Meteorological Society*, 28(11), 1493-1505. https://doi.org/10.1002/joc.1646

Marin, M., Feng, M., Phillips, H. E., & Bindoff, N. L. (2021). A global, multiproduct analysis of coastal marine heatwaves: Distribution, characteristics, and long-term trends. *Journal of Geophysical Research: Oceans*, *126*(2), e2020JC016708.

McCarthy, M., Christidis, N., Dunstone, N., Fereday, D., Kay, G., Klein-Tank, A., Lowe, J., Petch, J., Scaife, A., & Stott, P. (2019). Drivers of the UK summer heatwave of 2018. *Weather*, *74*(11), 390-396. https://doi.org/10.1002/wea.3628

Met Office (2018). Summer 2018. https://www.metoffice.gov.uk/binaries/content/assets/metofficegovuk/pdf/weather/learn-about/uk-past-events/interesting/2018/summer-2018---met-office.pdf

Météo-France (2018). Bilan climatique de l'été 2018. https://meteofrance.fr/sites/meteofrance.fr/files/files/editorial/Bilan-climatique-annee2018.pdf

Mieszkowska, N., Burrows, M., & Sugden, H. (2020). Impacts of climate change on intertidal habitats, relevant to the coastal and marine environment around the UK. *MCCIP Science Review 2020*, 256-271. https://doi.org/10.14465/2020.arc12.ith

Müller, H., Blanke, B., Dumas, F., & Mariette, V. (2010). Identification of typical scenarios for the surface Lagrangian residual circulation in the Iroise Sea. Journal of Geophysical Research: Oceans, 115(C7).

Norris, J., Vaughan, G., & Schultz, D. M. (2013). Snowbands over the English Channel and Irish Sea during cold-air outbreaks. *Quarterly Journal of the Royal Meteorological Society*, *139*(676), 1747-1761. https://doi.org/10.1002/qj.2079

Oh, H., Kim, G. U., Chu, J. E., Lee, K., & Jeong, J. Y. (2023). The record-breaking 2022 long-lasting marine heatwaves in the East China Sea. *Environmental Research Letters*, *18*(6), 064015.

Oliver, E. C., Donat, M. G., Burrows, M. T., Moore, P. J., Smale, D. A., Alexander, L. V., ... & Wernberg, T. (2018). Longer and more frequent marine heatwaves over the past century. *Nature communications*, *9*(1), 1-12.

Oliver, E. C. J., Burrows, M. T., Donat, M. G., Sen Gupta, A., Alexander, L. V., Perkins-Kirkpatrick, S. E., Benthuysen, J. A., Hobday, A. J., Holbrook, N. J., Moore, P. J., Thomsen, M. S., Wernberg, T., & Smale, D. A. (2019). Projected Marine Heatwaves in the 21st Century and the Potential for Ecological Impact. *Frontiers in Marine Science*, 6(December), 1–12. https://doi.org/10.3389/fmars.2019.00734

Plecha, S., & Soares, P. M. M. (2020) Global marine heatwave events using the new CMIP6 multi-model ensemble: from shortcomings in present climate to future projections, *Environmental Research Letters*, 15 (12), 124058. https://doi.org/10.1088/1748-9326/abc847

Plecha, S. M., Soares, P. M. M., Silva-Fernandes, S. M., & Cabos, W. (2021). On the uncertainty of future projections of Marine Heatwave events in the North Atlantic Ocean. *Climate Dynamics*, 56, 2027–2056. https://doi.org/10.1007/s00382-020-05529-3

Poppeschi, C., Charria, G., Goberville, E., Rimmelin-Maury, P., Barrier, N., Petton, S., Unterberger, M., Grossteffan, E., Repecaud, M., Quemener, L., Theetten, S., Le Roux, J.-F. & Tréguer, P. (2021). Unraveling salinity extreme events in coastal environments: A winter focus on the bay of brest. Frontiers in Marine Science, 8, 705403. https://doi.org/10.3389/fmars.2021.705403

Poppeschi, C., Charria, G., Daniel, A., Verney, R., Rimmelin-Maury, P., Retho, M., Goberville, E., Grossteffan, E., & Plus, M. (2022). Interannual variability of the initiation of the phytoplankton growing period in two French coastal ecosystems. *Biogeosciences*, 19, 5667–5687. https://doi.org/10.5194/bg-19-5667-2022

Reynolds R W, Smith T M, Liu C, Chelton D B, Casey K Sand Schlax M G 2007 Daily high-resolution-blended analyses for sea surface temperature, *J. Clim*. 20 5473–96

Ruthrof, K. X., Breshears, D. D., Fontaine, J. B., Froend, R. H., Matusick, G., Kala, J., Miller, B. P., Mitchell, P. J., Wilson, S. K., van Keulen, M., Enright, N. J., Law, D. J., Wernberg, T., & Hardy, G. E. S. J. (2018). Subcontinental heat wave triggers terrestrial and marine, multi-taxa responses. *Scientific Reports*, 8(1), 1–9. https://doi.org/10.1038/s41598-018-31236-5

Savu, A. (2022). Temperature Highs, Climate Change Salience, and Eco-Anxiety: Early Evidence from the 2022 United Kingdom Heatwave. *Climate Change Salience, and Eco-Anxiety*

Sims, D. W., Wearmouth, V. J., Genner, M. J., Southward, A. J., & Hawkins, S. J. (2004). Low-temperature-driven early spawning migration of a temperate marine fish. *Journal of Animal Ecology*, *73*(2), 333-341.

Smale, D. A., Wernberg, T., Oliver, E. C. J., Thomsen, M., Harvey, B. P., Straub, S. C., Burrows, M. T., Alexander, L. V., Benthuysen, J. A., Donat, M. G., Feng, M., Hobday, A. J., Holbrook, N. J., Perkins-Kirkpatrick, S. E., Scannell, H. A., Sen Gupta, A., Payne, B. L., & Moore, P. J. (2019). Marine heatwaves threaten global biodiversity and the provision of ecosystem services. *Nature Climate Change*, 9(4), 306–312. https://doi.org/10.1038/s41558-019-0412-1

Seuront, L., Nicastro, K. R., Zardi, G. I., & Goberville, E. (2019). Decreased thermal tolerance under recurrent heat stress conditions explains summer mass mortality of the blue mussel Mytilus edulis. *Scientific Reports*, *9*(1), 1–14. https://doi.org/10.1038/s41598-019-53580-w

Schlegel R.W., E.C.J. Oliver, T. Wernberg, A.J. Smit (2017) Nearshore and offshore co-occurrence of marine heatwaves and cold-spells, *Progress in Oceanography*, 151, 189-205. https://doi.org/10.1016/j.pocean.2017.01.004

Schlegel, R. W., Darmaraki, S., Benthuysen, J. A., Filbee-Dexter, K., Oliver, E. C. J. (2021) Marine cold-spells, *Progress in Oceanography*, 198, 102684. https://doi.org/10.1016/j.pocean.2021.102684

Simon, A., Plecha, S. M., Russo, A., Teles-Machado, A., Donat, M. G., Auger, P. A., & Trigo, R. M. (2022). Hot and cold marine extreme events in the Mediterranean over the period 1982-2021. *Frontiers in Marine Science*, *9*(August), 1–12. https://doi.org/10.3389/fmars.2022.892201

Southward, A. J. (1960). On changes of sea temperature in the english channel. *Journal of the Marine Biological Association of the United Kingdom*, *39*(3), 449–458. https://doi.org/10.1017/S0025315400013473

Wang, Y., Kajtar, J. B., Alexander, L. V., Pilo, G. S., & Holbrook, N. J. (2022). Understanding the changing nature of marine cold-spells. *Geophysical Research Letters*, 49, e2021GL097002. https://doi.org/10.1029/2021GL097002

Wethey, D. S., & Woodin, S. A. (2022). Climate change and Arenicola marina: Heat waves and the southern limit of an ecosystem engineer. *Estuarine, Coastal and Shelf Science*, *276*(December 2021), 108015. https://doi.org/10.1016/j.ecss.2022.108015

Wernberg, T., Bennett, S., Babcock, R. C., De Bettignies, T., Cure, K., Depczynski, M., Dufois, F., Fromont, J., Fulton, C. J., Hovey, R. K., Harvey, E. S., Holmes, T. H., Kendrick, G. A., Radford, B., Santana-Garcon, J., Saunders, B. J., Smale, D. A., Thomsen, M. S., Tuckett, C. A., Tuya, F., Vanderklift, M. A., & Wilson, S. (2016). Climate-driven regime shift of a temperate marine ecosystem. *Science*, 353(6295), 169–172. https://doi.org/10.1126/science.aad8745

Vogel, M. M., Zscheischler, J., Wartenburger, R., Dee, D., & Seneviratne, S. I. (2019). Concurrent 2018 hot extremes across Northern Hemisphere due to human-induced climate change. *Earth's future*, *7*(7), 692-703. https://doi.org/10.1029/2019EF001189

Yao, Y., Wang, C., & Fu, Y. (2022). Global Marine Heatwaves and Cold-Spells in Present Climate to Future Projections. *Earth's Future*, *10*(11), e2022EF002787.

Yiou, P., Cattiaux, J., Faranda, D., Kadygrov, N., Jézéquel, A., Naveau, P., Ribes, A., Robin, Y., Thao, S., Oldenborgh, G. J. & Vrac, M. (2020). Analyses of the Northern European summer heatwave of 2018. *Bulletin of the American Meteorological Society*, *101*(1), S35-S40. https://doi.org/10.1175/BAMS-D-19-0170.1ff.

Supplementary files

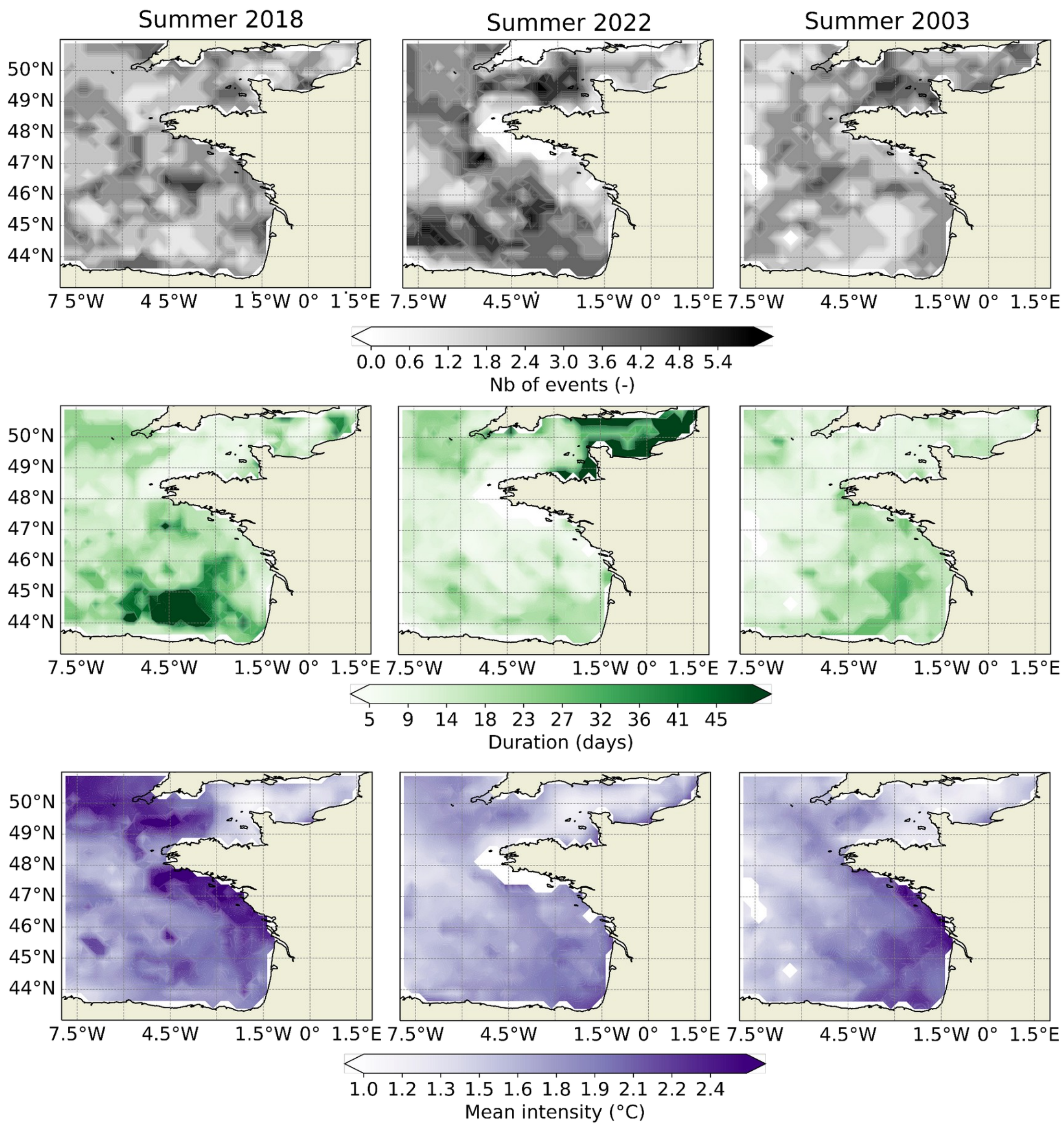

Figure S1: Summer (JJAS) number of events (first row), average duration (second row; in days) and average intensity (third row; in °C) for the top 3 summer in term of total activity in the whole domain (from left to right)

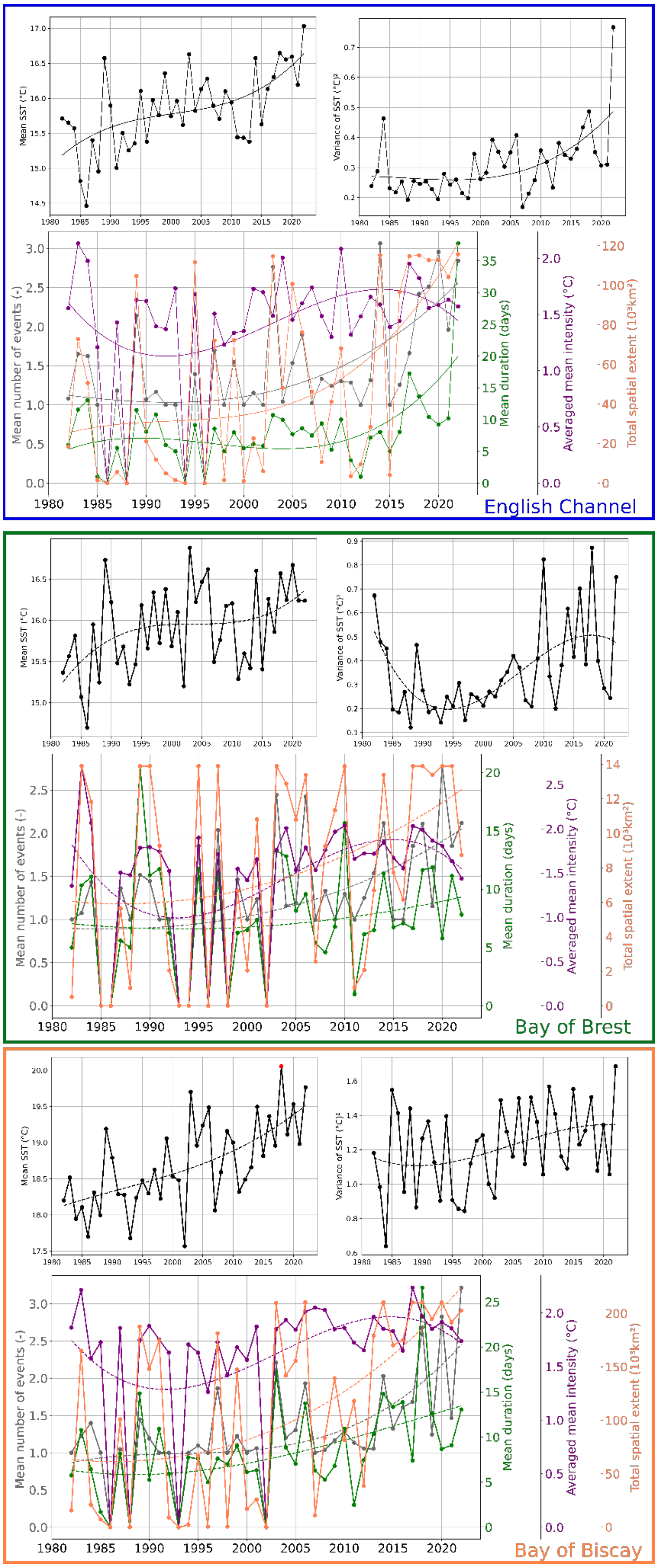

Figure S2: Same as for Figure 3 for summer MHWs but for three subregions: the English Channel (top), the Bay of Brest (middle) and the Bay of Biscay (bottom).

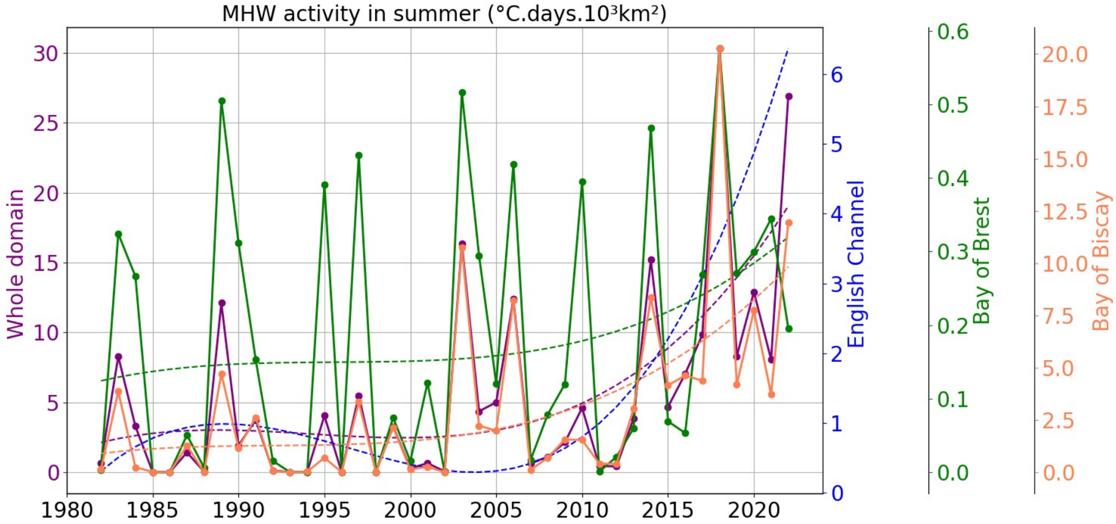

Figure S3: Time series of summer (JJAS) MHWs activity (°C.days.10³km²) for the whole domain (purple curve), the English Channel (blue curve), the Bay of Brest (green curve) and the Bay of Biscay (orange curve). Dash lines represent the regression of a third-order polynomial of the solid line with the same color.

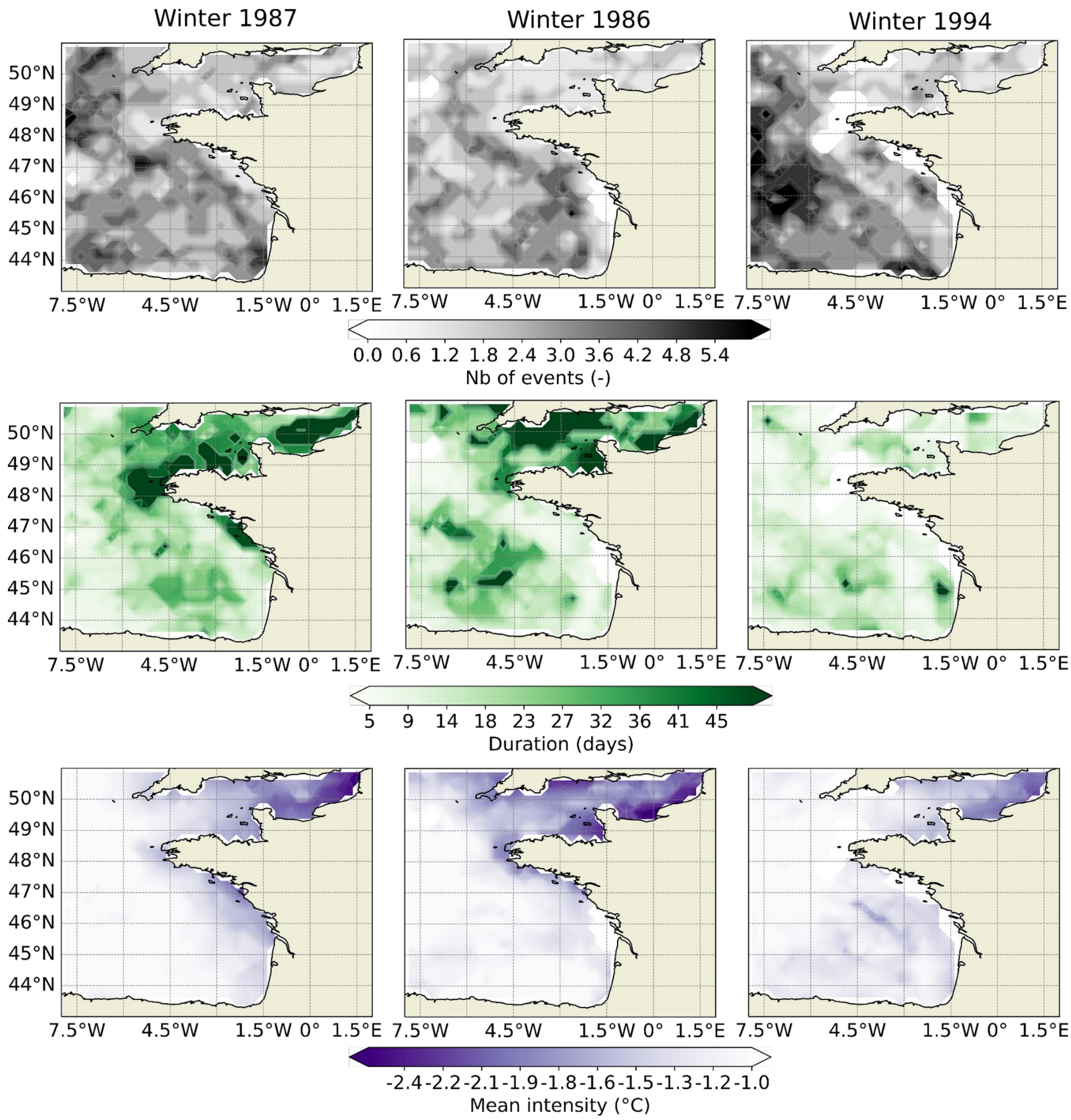

Figure S4: Same as Figure S1 but for MCSs in winter (DJFM).

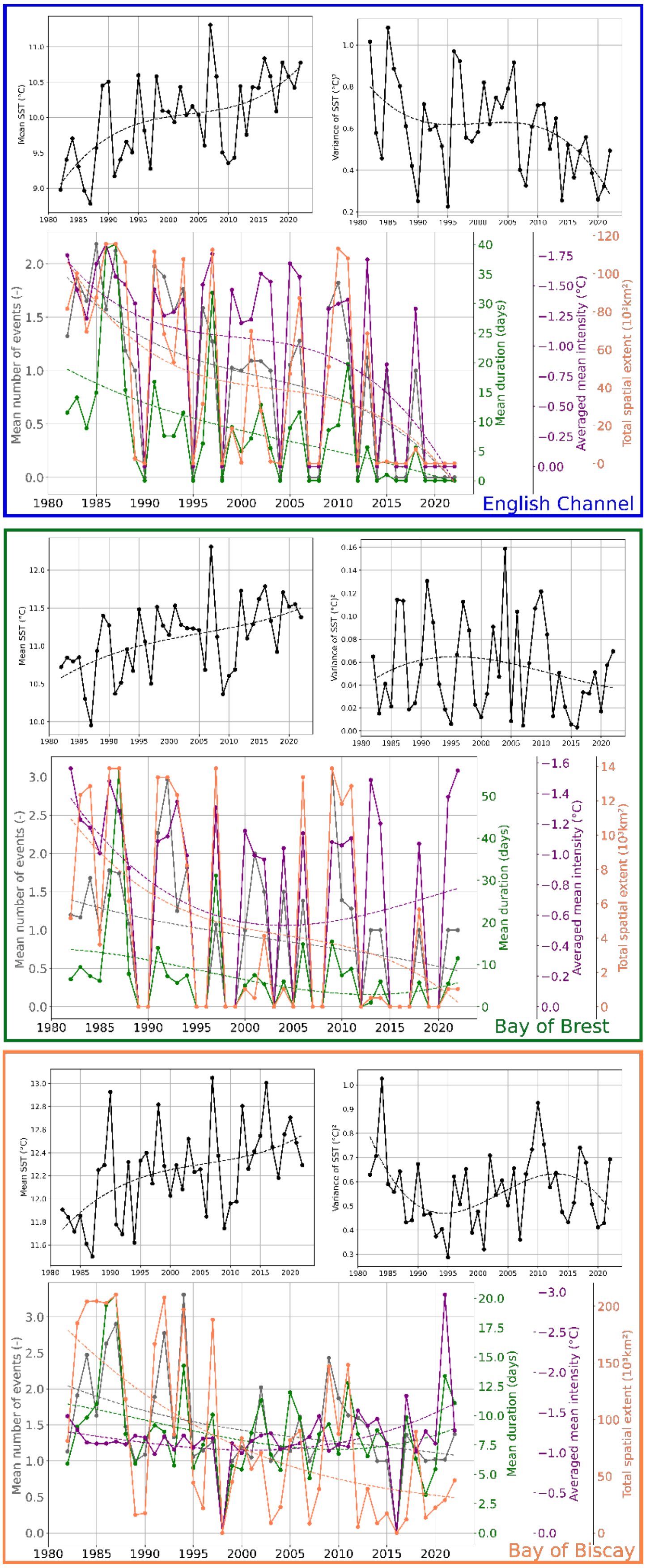

Figure S5: Same as Figure S2 but in winter (DJFM) and MCSs (blue curve).

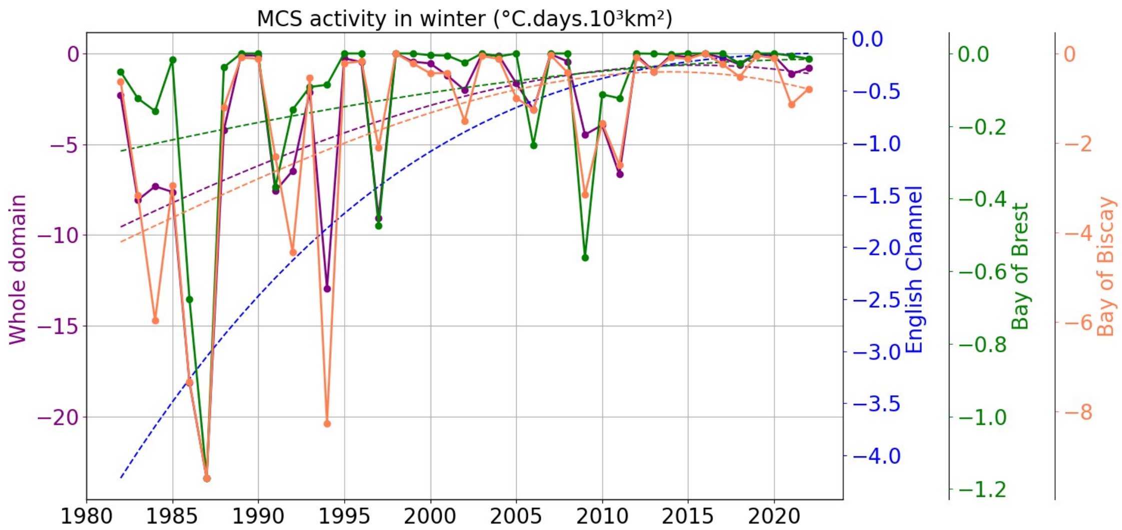

Figure S6: Same as for Figure S3 but for winter (DJFM) MCSs

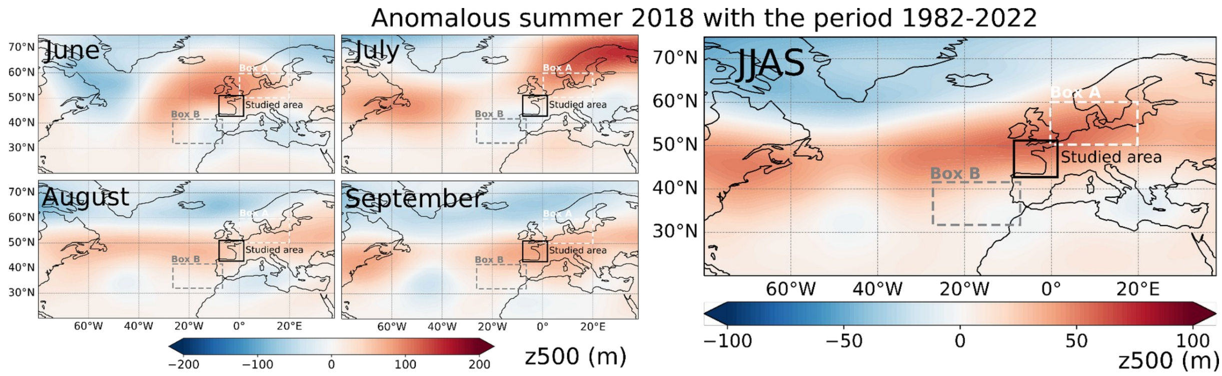

Figure S7: Anomalous geopotential height at 500 hPa (left panel) in June (top-left), July (top-right), August (bottom-left) and September (bottom-right) and June to September with the period 1982-2022 (right panel). Box A is the domain 0E20E-50N60N and box B is the domain 33W13W-31N41N.

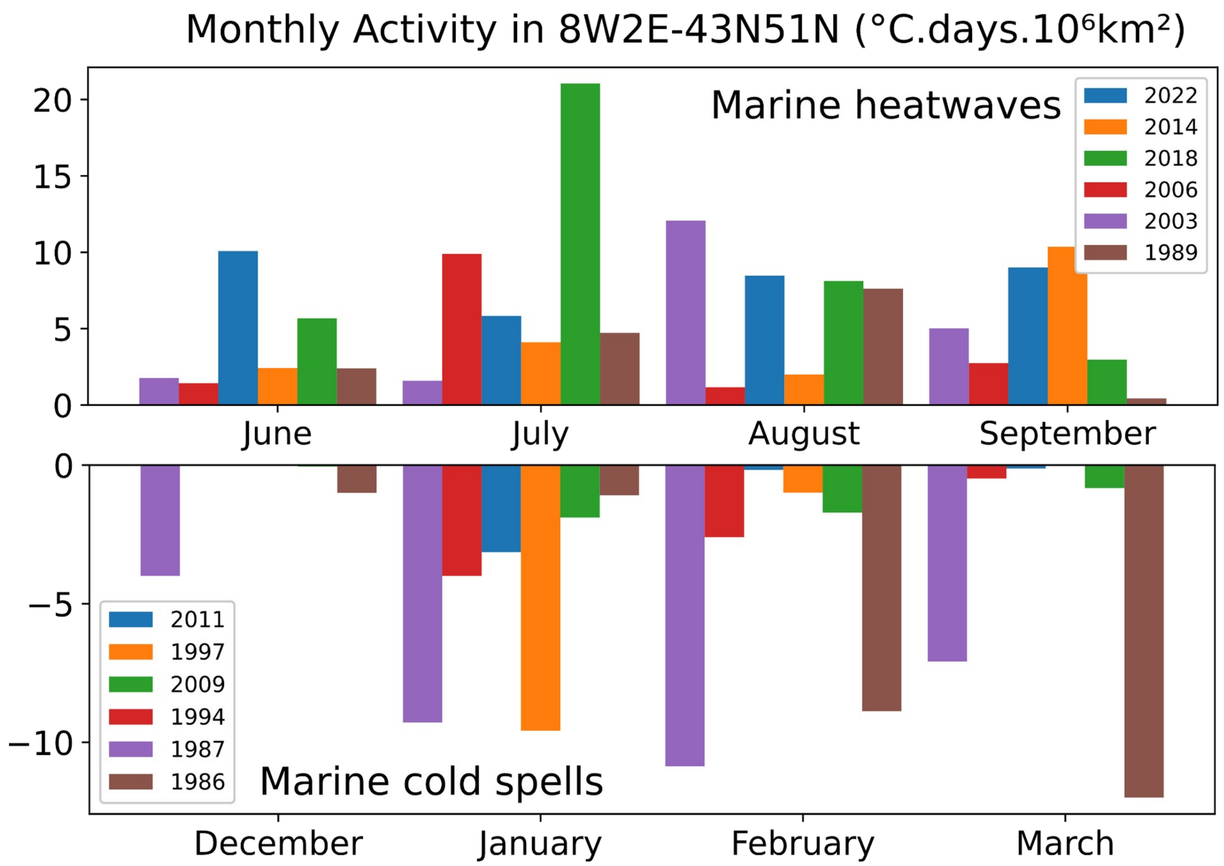

Figure S8: Total monthly activity in the Northeast Atlantic studied area (8W2E-43N51N) for marine heatwaves in summer months (top) and for marine cold-spells in winter months (bottom).

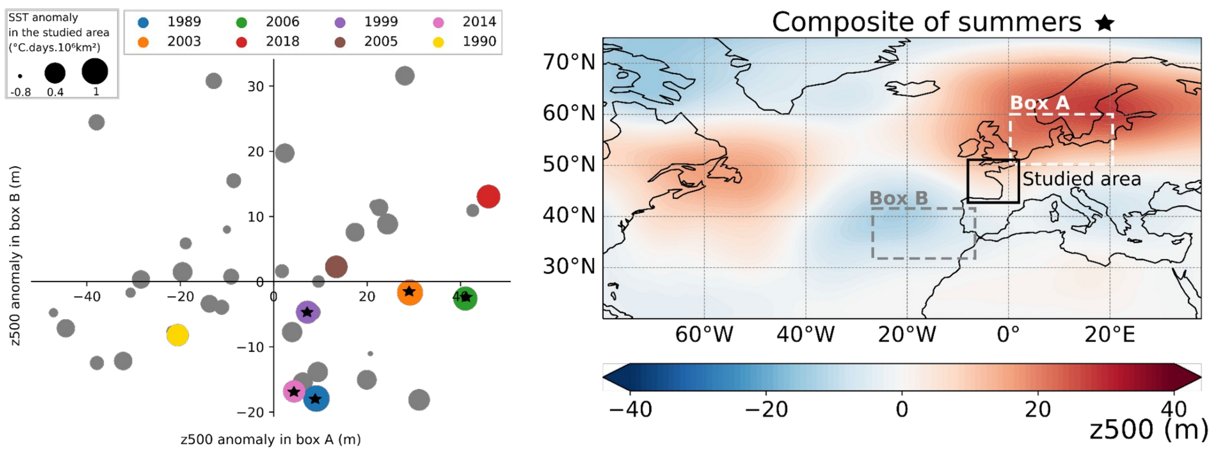

Figure 9: Same as Figure 8 but with SST instead of marine heatwave activity. SST anomalies are calculated with respect to the third-order trend (black dotted line in the top panel Figure 3). Coloured mark summer is for anomalous SST averaged of the studied area exceeding 0.4 ºC.

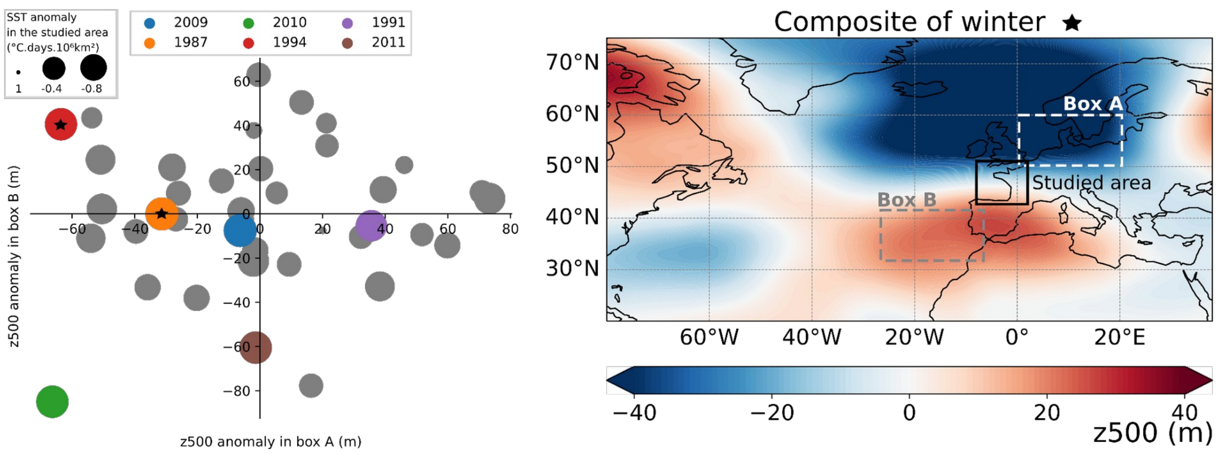

Figure S10: Same as Figure 9 but with SST instead of marine cold-spells activity. SST anomalies are calculated with respect to the quadratic trend (black dotted line in the top panel Figure 6). The colored mark winter is for anomalous SST averaged of the studied area below -0.4 ºC. Box A is the domain 0E20E-50N60N and box B is the domain 33W13W-31N41N.

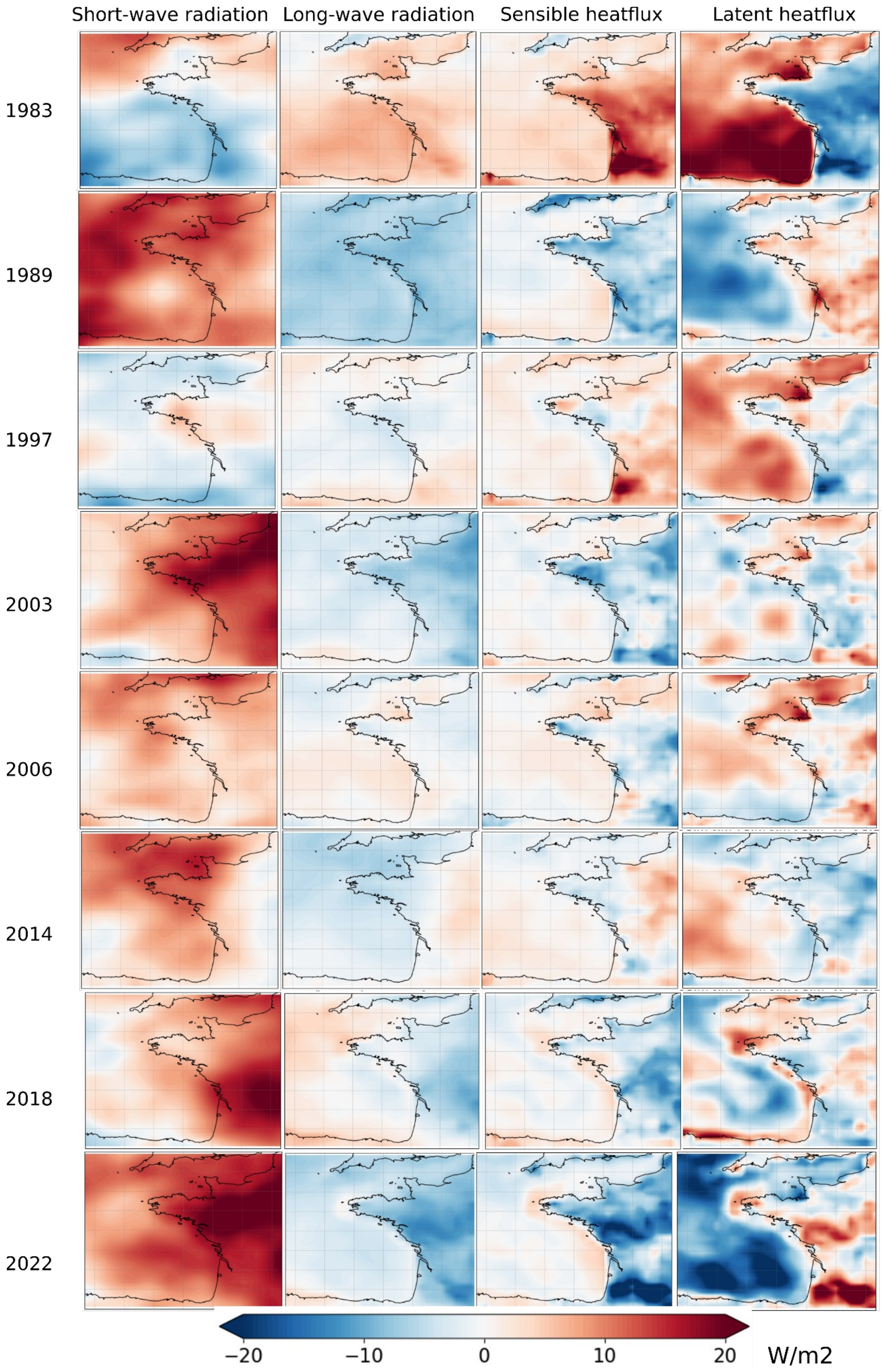
Short-wave radiation
Long-wave radiation
Sensible heatflux
Latent heatflux
1983
1989
1997
2003
2006
2014
2018
2022
−20
−10
0
10
20
W/m2

Figure S11: Anomalous short-wave radiation (first column; W/m2), long-wave radiation (second column; W/m2), sensible heat flux (third column; W/m2) and latent heat flux (fourth column; W/m2) compared to the period 1982-2022 for the eight most severe interannual summer (JJAS) MHWs. Positive fluxes are downward.

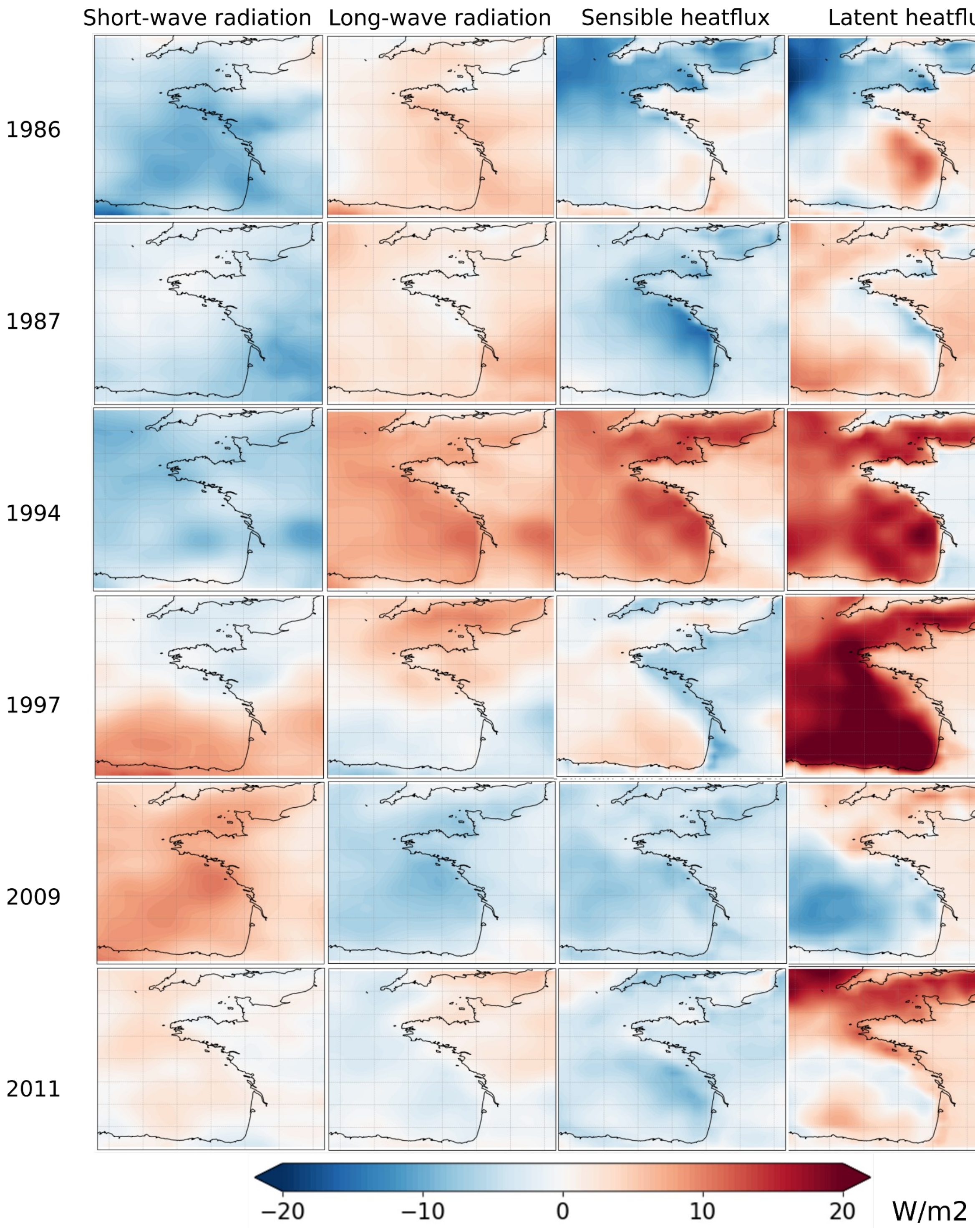

Figure S12: Same as Figure S13 but for the six most severe interannual winter MCSs.

Buoy names	Coordinates	Start acquisition
CARNot	1.56°E, 50.74°N	2004
GREENwich	0.04°E, 50.41°N	2006
SMILe	0.30°W, 49.34°N	2015
CHANnel	2.86°W, 49.90°N	1991
L4_Q	4.13°W, 50.15°N	2009
SEVEn stones	6.07°W, 50.09°N	1995
ASTAn	3.93°W, 48.77°N	2015
IROIse	4.55°W, 48.35°N	2000
SMARt	4.33°W, 48.31°N	2016
MOLIt	2.65°W, 47.46°N	2008
ARCAchon	1.23°W, 44.63°N	2017
BILBao	3.14°W, 43.41°N	2004
GIJOn	5.68°W, 43.64°N	2004

Table S1: Characteristics of the 13 *in situ* measurement buoys. Buoys indicated in blue are located in the English Channel, in green in the Bay of Brest and in orange in the Bay of Biscay.

Summer MHWs	Number of events (-)	Duration (days)	Mean intensity (°C)
Northeast Atlantic	1.4	8.9	1.7
English Channel	1.4	8.0	1.4
Bay of Brest	1.2	7.3	1.5
Bay of Biscay	1.3	8.3	1.6

Table S2: Mean properties (number of events, duration, mean intensity) of summer (JJAS) MHWs over the period 1982-2022 in the Northeast Atlantic, English Channel, Bay of Brest and Bay of Biscay

Winter MCSs	Number of events (-)	Duration (days)	Mean intensity (°C)
Northeast Atlantic	1.4	9.1	-1.4
English Channel	0.9	8.3	-1.0
Bay of Brest	0.9	7.0	-0.7
Bay of Biscay	1.4	8.4	-1.2

Table S3: Same as Table S2 but for winter (DJFM) MCSs